CHALMERS
UNIVERSITY OF TECHNOLOGY

Next Generation Thermal Management System Control Architecture for Battery Electric Vehicles

Master's thesis in Mobility Engineering

Karthik Hudugur Sathyanarayana
Punit Chandrappa

DEPARTMENT OF MECHANICAL ENGINEERING
CHALMERS UNIVERSITY OF TECHNOLOGY
Gothenburg, Sweden 2026
www.chalmers.se

Master's thesis 2026

Next Generation Thermal Management System Control Architecture for Battery Electric Vehicles

Karthik Hudugur Sathyanarayana
Punit Chandrappa

CHALMERS
UNIVERSITY OF TECHNOLOGY

Department of Mechanical Engineering
Chalmers University of Technology
Gothenburg, Sweden 2026

Next Generation Thermal Management System Control Architecture for Battery Electric Vehicles

Supervisor: Juan Antonio Moreno Gómez, Volvo Cars
Examiner: Petter Dahlander, Department of Mechanical Engineering

Master's Thesis 2026
Department of Mechanical Engineering
Chalmers University of Technology
SE-412 96 Gothenburg
Telephone +46 31 772 1000

Cover: Next Generation Thermal Management System Control Architecture for Battery Electric Vehicles.

Typeset in LaTeX
Printed by Chalmers Reproservice
Gothenburg, Sweden 2026

Next Generation Thermal Management System Control Architecture for Battery Electric Vehicles
Karthik Hudugur Sathyanarayana,
Punit Chandrappa
Department of Mechanical Engineering
Chalmers University of Technology

Abstract

The global automotive sector is experiencing a rapid transition towards electrification due to increasing concern over global warming and stricter emission regulations. Battery Electric vehicles (BEVs) play a central role in this transition. The efficiency and reliability of BEVs largely depend on the thermal behavior of various temperature-dependent components like battery pack, electric motor, and power electronics. The thermal management system (TMS) must not only balance the cooling and heating of temperature critical components, but also ensure passenger comfort by regulating the cabin temperature as per the need.

There are several TMS architectures used in the automotive application. The key focus of this study will be investigating the performance of Full Secondary Loop (FSL) architecture which uses propane-based refrigerant and water-glycerol as coolant. The investigation in this project has been done using the Complete Vehicle Thermal Modelling (CVTM) simulation environment at Volvo Cars, which is a GT-Suite based one-dimensional (1D) thermal-fluid model that represents the physical FSL hardware.

The study focuses on investigating the effectiveness of the FSL architecture in controlling the temperature of battery, electric drivetrain and cabin temperature in an energy efficient manner by studying the effects of operating parameters of various actuators present in a TMS like pumps, valves, radiator fan and compressor. A control strategy has also been developed based on the requirements for cooling of the battery, electric drivetrain or cabin and the operating parameters of the controllable actuators.

The results demonstrate that a properly designed FSL system can effectively regulate the temperatures of critical components and the cabin, and also identifies the optimal operating parameters necessary for efficient system performance.

Keywords: Battery Electric Vehicle (BEV), Thermal Management System (TMS), Full Secondary Loop (FSL), Complete Vehicle Thermal Modelling (CVTM), One Dimensional (1D).

Acknowledgements

We would like to express our sincere gratitude to all those who supported and guided us throughout the completion of this thesis work titled *"Next Generation Thermal Management System Control Architecture for Battery Electric Vehicles"*.

We are deeply thankful to our guide and supervisor Juan Antonio Moreno Gómez, Volvo Cars, for his continuous guidance, valuable suggestions, technical support, and encouragement during the course of this work. His insights and expertise greatly contributed to the successful completion of this study.

We would also like to extend our sincere thanks to Helena Martini, Babak Heydarnezhad, Hamed Jamshidi, Rangakishen Mavanur Sampath, Mukund Rudravajhala and also other people at Volvo for their valuable discussions, technical support, encouragement, and guidance throughout the project duration. We further acknowledge the support of the organization and technical teams for providing access to simulation tools, technical discussions, and continuous assistance related to the development of the Full Secondary Loop (FSL) thermal management control architecture and the GT-SUITE simulation environment.

We would also like to express our sincere gratitude to Professor Petter Dahlander and the faculty members of the Department of Mechanical Engineering at Chalmers University of Technology for their academic guidance, support, and the resources provided throughout this Master Thesis work.

We sincerely acknowledge our family members, friends and colleagues for their continuous support, encouragement, patience, and unwavering motivation throughout the project duration and our academic journey.

Karthik Hudugur Sathyanarayana, Punit Chandrappa, Gothenburg, May 2026

Nomenclature

Below is the nomenclature of abbreviations, parameters and variables.

Abbreviations

BEV	Battery Electric Vehicle
CO_2	Carbon dioxide
COP	Coefficient of Performance
CVTM	Complete Vehicle Thermal Model
DOE	Design of Experiments
DX	Direct Expansion
ED	Electric Drive
EDU	Electric Drive Unit
FSL	Full Secondary Loop
GWP	Global Warming Potential
HFC	Hydrofluorocarbon
HFO	Hydrofluoroolefin
HV	High Voltage
HVAC	Heating, Ventilation, and Air Conditioning
ICE	Internal Combustion Engine
iCond	Internal Condenser
ODP	Ozone Depletion Potential
PFAS	Per- and Polyfluoroalkyl Substances
R290	Propane refrigerant
R744	Carbon dioxide refrigerant
SSL	Semi-Secondary Loop
TMS	Thermal Management System
VMA	Valve Module Assembly

WCond	Water-Cooled Condenser
WLTC	Worldwide Harmonized Light Vehicle Test Cycle

Parameters

$COP_{battery}$	Coefficient of performance during battery cooling
COP_{cabin}	Coefficient of performance during cabin cooling
$COP_{combined}$	Coefficient of performance during combined cooling
$E_{compressor}$	Compressor energy consumption
E_{fan}	Radiator cooling fan energy consumption
E_{pump}	Pump energy consumption
E_{total}	Total auxiliary energy consumption
I	Battery current
$Q_{battery}$	Heat absorbed from battery
Q_{cabin}	Heat absorbed from cabin
R	Battery internal resistance
T_{amb}	Ambient temperature
$T_{battery}$	Battery average temperature
$T_{battery\,initial}$	Initial battery temperature
T_{cabin}	Cabin air temperature
$T_{cabin\,initial}$	Initial cabin temperature
$t_{cooling\,battery}$	Battery cooling time
$t_{cooling\,cabin}$	Cabin cooling time
ΔT	Battery temperature spread

Variables

PWM	Pulse Width Modulation operating condition
h	Convective heat transfer coefficient
A	Heat transfer area
Q	Heat transfer rate

Contents

List of Figures

List of Tables

1

Introduction

1.1 Background

The global automotive sector is undergoing a rapid transformation towards electrification. The major driver for this transformation is the tighter emission standards and regulations set by the government to meet the climate targets. To fulfill the average fleet CO_2 emission requirements and to avoid financial penalties, automakers are adopting towards Battery Electric Vehicles (BEVs) as an effective strategy. According to the Global EV Outlook 2025, global electric car sales reached approximately 17 million units in 2024. This growth has continued into 2025, with more than 4 million electric cars sold in the first quarter alone, representing an increase of about 35% compared to the same period in 2024 [1].

With the increasing adoption of BEVs, ensuring reliable and efficient operation has become a critical task and also an engineering challenge. Compared to Internal Combustion Engine (ICE) vehicles, BEVs are far more sensitive to temperature fluctuations. ICE vehicles contain predominantly mechanical parts that are designed to withstand high operating temperatures, often exceeding 100°C, without significant performance degradation. In contrast, BEVs rely on temperature critical components like lithium-ion batteries, power electronics and electric motors, all of these components operate efficiently only within a narrow thermal range. Deviations from this optimal range can result in reduced battery efficiency, cell ageing and even safety risks such as thermal runaway. These thermally dependent limitations of the components also directly influence the driving range of the vehicle, particularly when driven in extreme climate conditions. In these conditions the temperature critical components should be either heated or cooled and the energy for doing this is drawn from battery itself, which further reduces the range of BEVs and increases the range anxiety among the customers [2].

Due to the above explained thermal dependent characteristics BEVs require a dedicated thermal management system to keep all critical components within their optimal thermal range and also to enhance the passenger comfort by regulating the Heating, Ventilation and Air Conditioning (HVAC) of the vehicle cabin.

1.2 Problem Statement

As competition intensifies among manufacturers to deliver vehicles with higher efficiency and long ranges, the ability to manage heat effectively has become a fundamental design priority in BEVs. Therefore, advanced cooling technologies, integrated multi-loop systems and heat pump architectures are now viewed as key contributors to enhance efficiency, reliability and increasing the component life of electric vehicles. In addition to performance requirements, emerging regulatory restrictions on per- and polyfluoroalkyl substances (PFAS) are driving the transition toward alternative refrigerants with lower environmental impact. One of the alternative solutions for the current refrigerant is Propane (R290), but the major concern is that propane is a highly flammable gas. This shift necessitates the adoption of advanced thermal management architectures that can effectively integrate new working fluids while ensuring safety and performance.

For all these underlying challenges, Full Secondary Loop (FSL) has emerges as a promising solution due to its capability to decouple refrigerant and coolant circuits, enabling indirect heat transfer and improved system flexibility. However, this increased flexibility introduces significant complexity in system control and operation. The thermal behavior of the system depends on multiple interacting components, including pumps, valves, heat exchangers, and air-side systems such as radiators and fans for enhancing air flow through heat exchangers.

Control actions such as pump speed variation, valve configurations, and radiator fan operation are interdependent and influence not only heat transfer performance but also energy consumption and system stability. Therefore, there is a need to systematically investigate how control parameters influence thermal behavior in full secondary loop systems and to identify suitable operating strategies for achieving effective and energy-efficient cooling under different operating conditions.

1.3 Envisioned Solution

To address the challenges associated with the control and operation of full secondary loop thermal management systems, this study proposes a simulation-based investigation of system-level thermal behavior and control strategies. A detailed system model representing a full secondary loop architecture, implemented within Volvo's internal Complete Vehicle Thermal Modelling (CVTM) framework and the GT-SUITE simulation environment, is used to investigate the thermal behavior of the system.

The approach involves defining multiple cooling operation modes based on operating conditions such as thermal load and ambient temperature. For each mode, appropriate coolant flow paths are established using valve configurations, and control strategies are implemented to regulate actuator behavior, including pump speeds, valve positions, and radiator fan operation.

A supervisory control strategy is employed to select suitable operating modes based on system conditions, while low-level control is used to ensure stable and efficient operation within each mode. The performance of the system is evaluated under varying operating scenarios to assess thermal effectiveness, energy efficiency, and system stability.

Through this approach, the study aims to identify optimal operating parameters and control strategies that enable effective temperature regulation of critical components while minimizing energy consumption.

1.4 Objectives

The objectives of this study are as follows:

1. To analyze the structure and functionality of a full secondary loop thermal management system for Battery Electric Vehicles using system-level simulation models.

2. To investigate the interaction between thermal subsystems and coolant circuits under cooling-dominated operating conditions.

3. To define and implement different cooling operation modes based on system requirements and operating conditions.

4. To identify suitable actuator operating strategies for pumps, valves, and radiator fan under different cooling modes.

5. To evaluate system performance in terms of thermal regulation, energy efficiency, and stability under varying thermal loads and ambient conditions.

1.5 Limitations

This study is subject to the following limitations:

1. The analysis is conducted entirely in a simulation environment using GT-SUITE and CVTM, and the results are not validated through experimental or vehicle-level testing.

2. The investigation is limited to full secondary loop architecture, and other thermal management configurations are not analyzed in detail for comparison.

3. Component aging, degradation effects, and long-term reliability are not considered within the scope of this work.

4. The study focuses primarily on cooling operation modes, while heating modes and heat recovery strategies are not explored in detail.

2

Theory

This chapter presents the theoretical background and previous research relevant to TMS in BEVs. It covers the thermal requirements of key vehicle subsystems, commonly used thermal management architectures and refrigerant selection reported in literature. The chapter concludes by identifying the research gap that motivates the present study.

2.1 Thermal Management in Battery Electric Vehicles

The thermal management system of a Battery Electric Vehicle is responsible for controlling heat generation, heat rejection, and heat distribution across multiple onboard subsystems. Unlike a single-purpose cooling system used in ICE vehicles, BEV thermal management must simultaneously support battery conditioning, electric drivetrain temperature control, power electronics protection, and cabin climate control. These functions are interdependent and must be coordinated under continuously changing operating conditions [3].

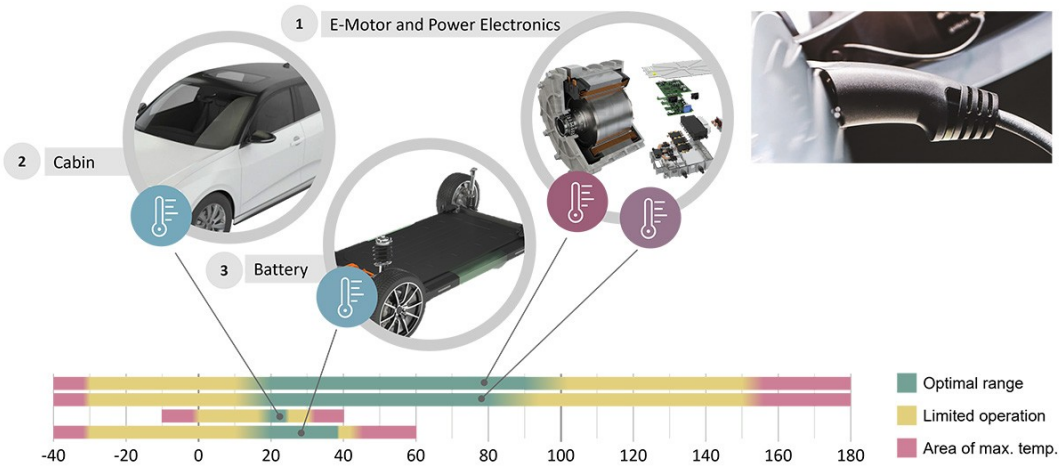

Figure 2.1: Optimum operating temperature of BEV components [5]

Heat in battery-electric vehicles arises from multiple components and external influences. The battery pack generates thermal energy because of internal resistance during both charging and discharging. The electric motor produces heat as a by-product of torque generation, while power electronics such as inverters, converters, and onboard chargers emit heat through switching and conduction losses. Cabin thermal loads are further affected by solar radiation, the number of occupants, and surrounding environmental conditions. The overall intensity of these thermal loads depends on factors like driving style, charging power, road conditions, and climate. [3] [4]. Figure 2.1 shows the optimal operating temperature of various components of a BEV that need to be managed by the TMS.

Table 2.1: Optimal operating temperature ranges of key EV components

Component	**Optimal Temperature Range (°C)**
Battery	20 – 40
E-Motor and Power Electronics	20 – 80
Cabin (Comfort)	20 – 25

2.1.1 Thermal Management of Battery

Lithium-ion batteries are widely used in modern electric vehicles due to their high energy and power density, strong energy storage capability, and ability to be recharged without memory-effect limitations. Despite these advantages, their thermal behavior remains a major concern. During discharge, internal electrochemical processes produce heat, which can rapidly increase cell temperature. For this reason, an efficient cooling system is necessary to prevent overheating and protect the battery from damage. On the other hand, when the battery operates below its recommended temperature range, issues such as reduced power output and faster aging can occur. As a result, an effective heating system is equally important to warm the battery to an appropriate operating temperature under cold conditions. [7]

In modern electric vehicles, liquid cooling is one of the most widely used methods for controlling battery temperature because of its high heat removal capability and better temperature uniformity.[7][8] Figure 2.2 shows the layered structure of an battery module. The battery cells are grouped into module and placed within the battery housing. The battery temperature control system is positioned beneath the module to remove heat or for heating during different operations. During battery cooling, the heat produced by the cells is transferred to the cooling plates, where the circulating coolant absorbs the thermal energy and is then directed towards the other components of thermal management system to reject the heat before being recirculated again.

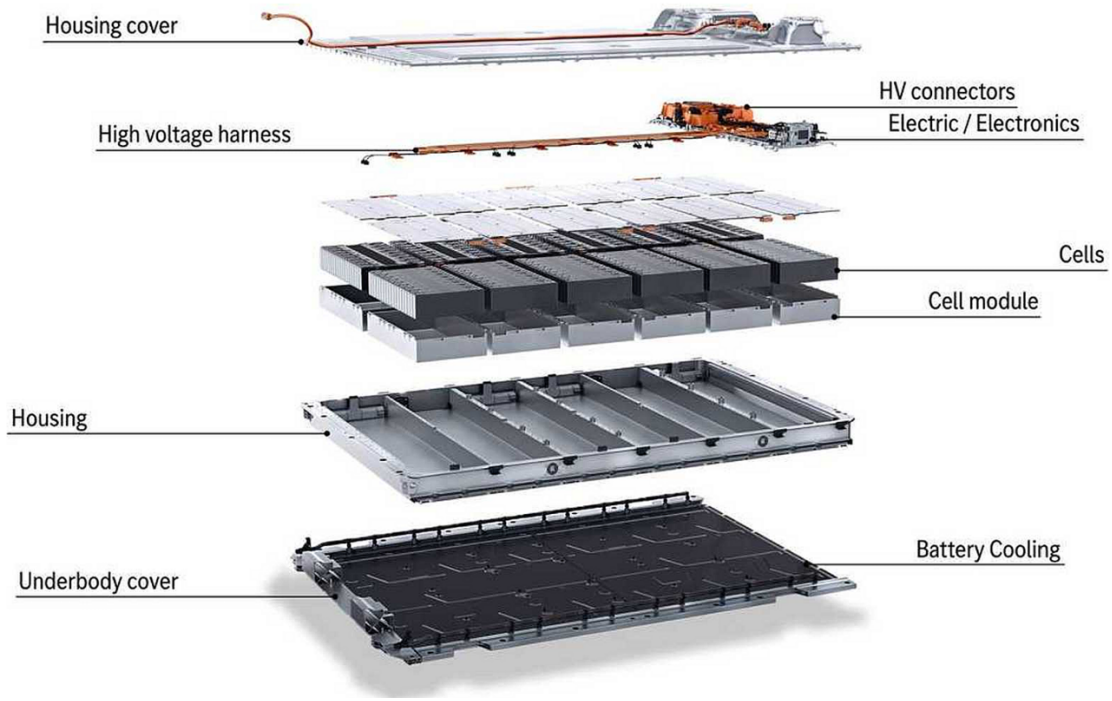

Figure 2.2: Liquid Cooling of Battery in BEV [8]

2.1.2 Thermal Management of Electric Drive Unit

The electric drive unit (EDU) in battery electric vehicles integrates key components such as the electric motor, power electronics (inverter), and transmission system. During operation, these components generate heat due to electrical, magnetic, and mechanical losses. If this heat is not effectively dissipated, it can negatively impact efficiency, reliability, and durability. Therefore, a well-designed thermal management system is essential to maintain the drive unit within its optimal operating temperature range.

Electric motors in BEVs are used to convert electrical energy received from battery to mechanical energy for propelling the vehicle. During this conversion, not all the input electrical energy is transferred to useful mechanical energy, some portion of it is dissipated as heat due to various losses as described in Figure 2.3. If the heat is not effectively controlled it may result in deterioration of insulation materials and potential damage to motor components.

The optimal operating temperature range of an electric drive unit is relatively wide compared to that of battery systems. This is because components such as the electric motor and power electronics are designed to withstand higher thermal loads and operate efficiently over a broader temperature band. This wider operating range provides greater flexibility in thermal management, allowing the system to tolerate temperature fluctuations without immediate performance loss. However, maintaining temperatures within an optimal band is still important to minimize losses, prevent overheating, and ensure long-term reliability of the electric drive unit.

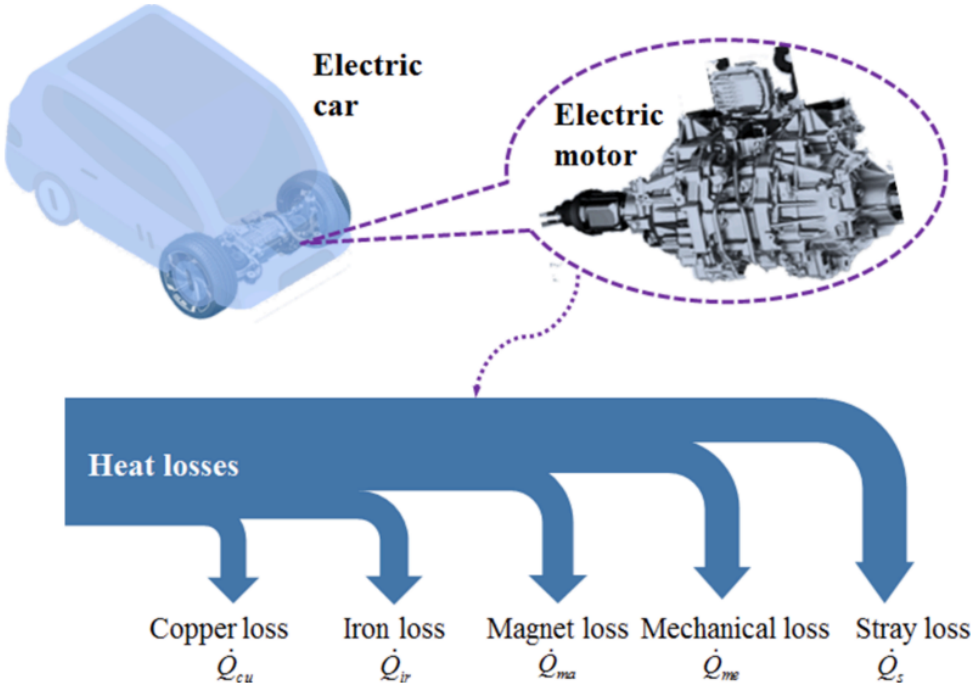

Figure 2.3: Various losses in electric motor resulting in heat generation [10]

2.1.3 Thermal Management of Cabin in Electric Vehicles

The thermal management of the passenger cabin in electric vehicles (EVs) is essential to ensure occupant comfort while minimizing energy consumption. Unlike conventional vehicles, where waste heat from the internal combustion engine can be used for cabin heating, EVs rely entirely on electrical energy from the battery for both heating and cooling. As a result, cabin thermal management has a direct impact on vehicle range and overall energy efficiency.

As illustrated in Figure 2.4 think of the car cabin like a closed room sitting in the sun. In a battery electric vehicle (BEV), keeping this space cool and comfortable is important, but it also consumes battery energy.

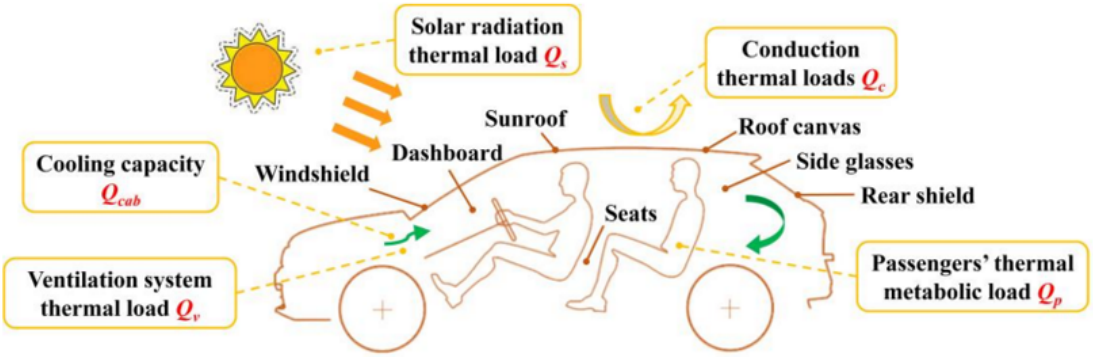

Figure 2.4: Sources of heat generation in car cabin [4]

The main source of heat is sunlight. Direct sunlight enters through the windows and heats up surfaces like the seats, dashboard, and floor. These surfaces then release heat back into the air, making the cabin even hotter. In addition, scattered sunlight from the sky (diffuse radiation) also contributes to heating. Heat also comes from the surroundings. When the outside temperature is high, heat flows into the cabin through the car body and roof by conduction. Inside the cabin, warm air moves and spreads heat due to convection. Ventilation brings outside air into the cabin, which can further increase the cooling load if the ambient air is hot.

All these heat sources together increase the cooling demand. Therefore, higher heat gain leads to higher energy consumption and reduced driving range. To ensure comfort, engineers follow guidelines from American Society of Heating, Refrigerating and Air-Conditioning Engineers (ASHRAE), which recommend maintaining a cabin temperature of about 20–25°C with proper airflow and humidity. This thesis primarily majorly focus on keeping the cabin temperature in this range, other comfort parameters such as humidity and airflow are not considered in the present analysis.

2.1.4 Components of TMS in Electric Vehicles

The key components of a thermal management system in BEVs include:

1. **Compressor**: The compressor serves as the primary driver of the refrigerant circuit. It draws in low-pressure vapor from the evaporator or chiller and compresses it to a high-pressure, high-temperature state. This elevated pressure level enables effective heat rejection in the condenser. Unlike conventional vehicles that rely on engine-driven compressors, BEVs use fully electric units, allowing operation independent of vehicle speed and providing more precise control over cooling performance.[4]

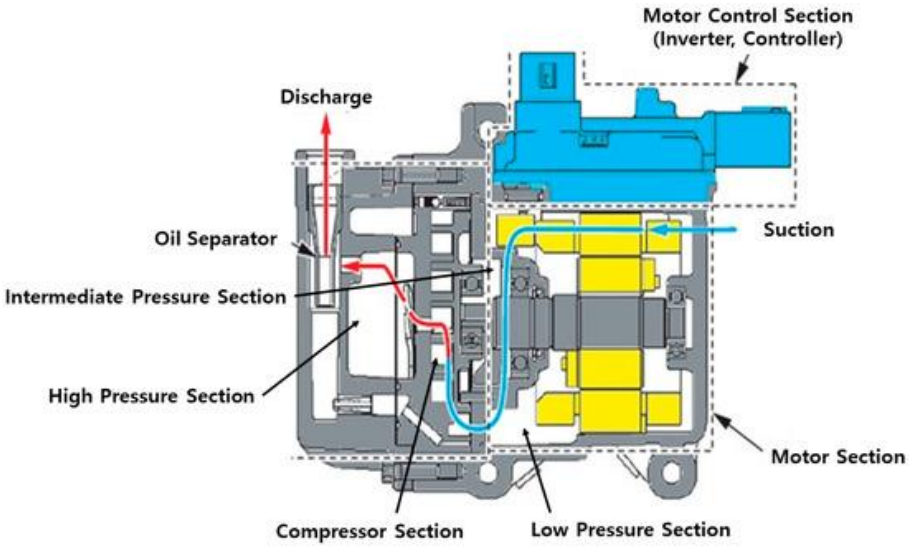

Figure 2.5: Electric scroll compressor used in HVAC system[9]

2. **Expansion Valve**: The expansion valve plays a vital role in the refrigerant circuit by lowering the refrigerant's pressure and temperature before it enters the evaporator or chiller. In addition to this pressure drop, the valve regulates the refrigerant flow rate, ensuring that the evaporator receives the correct amount of refrigerant for effective heat absorption and stable system performance.

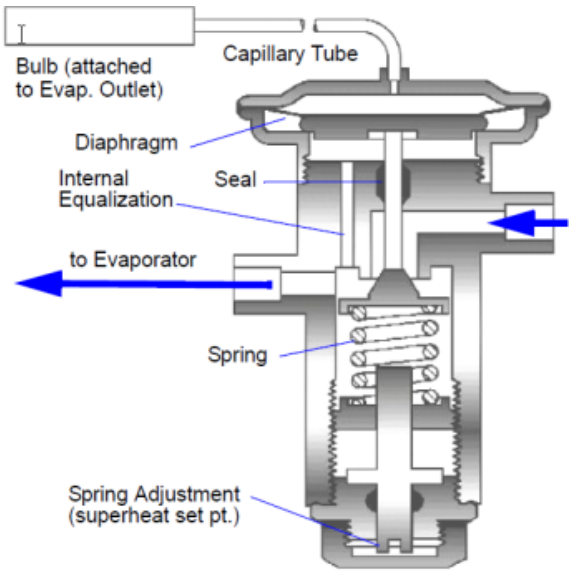

Figure 2.6: Thermal Expansion Valve[16]

3. **Heat Exchangers**: Heat exchangers are key elements of a battery electric vehicle thermal management system because they allow heat to be taken from one fluid or component and transferred to another medium without the fluids mixing. They are used at different points in the system depending on whether

heat must be removed or supplied. For example, a chiller transfers heat from the coolant loop to the refrigerant, which helps lower the temperature of the battery or electric drive unit coolant. A condenser or water-cooled condenser allows the refrigerant to release heat to air or another coolant loop. Similarly, a radiator acts as a medium of heat exchange between the coolant loop and the ambient environment, while the cabin evaporator absorbs heat from the passenger compartment during cooling operation. In this way, heat exchangers support both heat absorption and heat rejection processes. Their effectiveness has a direct influence on cooling performance, energy consumption, and the ability to maintain the battery, electric drive unit, and cabin within their required temperature limits. [4]

4. **Pumps**: Pumps are essential components in the coolant-based thermal management system of battery electric vehicles because they circulate the coolant through different thermal loops. The coolant pump ensures that heat absorbed from components such as the battery pack, electric drive unit, and power electronics is continuously transported to heat exchangers such as radiators, chillers, or water condensers. In modern BEVs, electric coolant pumps are commonly used because their speed can be controlled according to cooling demand. By adjusting the pump speed, the system can regulate coolant flow rate, improve heat transfer, and reduce unnecessary energy consumption. Therefore, pump operation has a direct influence on cooling performance, temperature uniformity, and overall system efficiency.

5. **Valves**: Valves are used in electric vehicle thermal management systems to control the direction and distribution of coolant or refrigerant flow between different components. They allow the system to switch between operating modes such as battery cooling, cabin cooling, cabin heating, or combined heat rejection. In integrated TMS, multi-port valves are often used to connect or isolate different thermal loops depending on the required operating condition. Proper valve control ensures that coolant is directed only to the components that require heating or cooling, improving energy efficiency and system response. As a result, valves play an important role in managing thermal flow paths and enabling flexible operation of complex BEV thermal management architectures.

2.1.5 Cooling Mechanisms in Electric Vehicle TMS

In BEVs, the thermal management of key components such as the battery, ED unit, and cabin is achieved through a combination of coolant-based and refrigerant-based systems. In current battery electric vehicles, coolant loops are predominantly used for the thermal management of the battery and electric drive unit, ensuring that these components operate within their optimal temperature range. On the other hand, the refrigerant loop is primarily utilized for the HVAC system, where it directly manages cabin thermal comfort. The refrigerant loop acts as an intermediate heat transfer mechanism between different coolant circuits. Specifically, the refrigerant system facilitates heat exchange between a cold coolant loop (connected to components

such as the battery and electric drive unit) and a hot coolant loop (connected to the heat rejection system). This interaction typically occurs through heat exchangers such as chillers and condensers, where the refrigerant absorbs heat from the cold coolant loop and subsequently rejects it to the hot coolant loop.

The Figure 2.7 illustrates the combined operation of the refrigerant cycle and its interaction with the coolant loop.

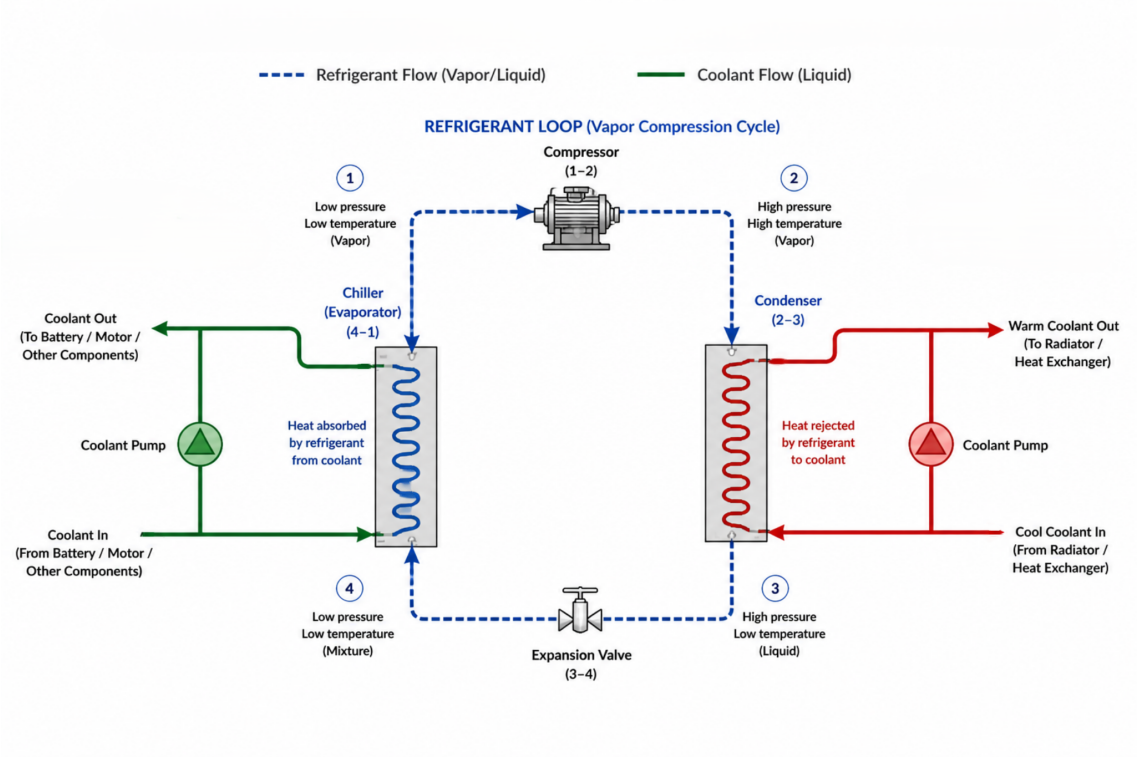

Figure 2.7: Refrigeration Cycle and Heat Transfer between Refrigerant and Coolant

The cycle begins with the refrigerant entering the compressor in a low-pressure, low-temperature vapor state (state 1). The compressor increases its pressure and temperature, producing a high-pressure, high-temperature vapor (state 2). This hot refrigerant then flows into the condenser, where it transfers heat to the coolant circulating on the heat rejection side. As heat is rejected, the refrigerant condenses into a high-pressure liquid (state 3), while the coolant carries this heat to the radiator or external environment. The high-pressure liquid refrigerant then passes through the expansion valve, where it undergoes a pressure drop, resulting in a low-pressure, low-temperature mixture (state 4). This cold refrigerant enters the chiller (evaporator), where it absorbs heat from the coolant circulating from the battery, electric drive unit, or other components. As heat is absorbed, the refrigerant evaporates back into a low-pressure vapor (state 1), completing the cycle.

2.2 Refrigerants Used in Automotive Systems

A wide range of refrigerants have been developed and used in automotive thermal management systems, each with different thermodynamic, environmental, and safety characteristics. Table 2.2 illustrates the properties of refrigerants commonly used in HVAC systems.

Table 2.2: Comparison of refrigerants used in automotive thermal management systems [12]

Property	**R134a**	**R1234yf**	**CO_2 (R744)**	**Propane (R290)**
Type	HFC	HFO	Natural	Natural hydrocarbon
GWP	∼1430	∼4	1	∼3
ODP	0	0	0	0
Flammability	A1 (Non-flammable)	A2L (Mild)	A1 (Non-flammable)	A3 (Highly flammable)
Operating Pressure	Moderate	Moderate	Very high	Moderate
Critical Temp (°C)	101	94.7	31	96.7
Performance	Good	Similar to R134a	Good (heat pump)	Excellent
Environmental Impact	High GWP	Low GWP, PFAS concern	Very low	Very low
Cost	Low	High	Moderate	Low
System Complexity	Low	Low	High	Moderate
Safety Concern	Low	Mild flammability	High pressure	High flammability
Current Use	Phased out	Widely used	Emerging	Limited (safety)

Among these, R134a was widely used in earlier automotive air conditioning systems due to its stable performance and compatibility with system components. However, its high global warming potential (GWP = 1430) led to its gradual phase-out under environmental regulations.[11]

To address this issue, R1234yf was introduced as a low-GWP alternative and has become the current industry standard in many battery electric vehicles. With a significantly lower GWP (=4), R1234yf offers similar thermodynamic performance to R134a and requires minimal system modifications.[11] In recent years, increasing attention has been directed towards the environmental impact of refrigerants, particularly those belonging to the group of PFAS. Since R1234yf falls under this category, emerging regulations aimed at restricting PFAS usage have raised concerns about its long-term viability. As a result, there is a growing need to identify alternative refrigerants that not only provide efficient thermal performance but also comply with future environmental and safety regulations. Therefore, the selection of refrigerants for automotive thermal management systems is evolving beyond performance considerations to include environmental sustainability, regulatory compliance, and system safety, driving ongoing research into next-generation

refrigerants.

In addition to synthetic refrigerants, natural refrigerants such as carbon dioxide (R744) are increasingly being explored for automotive applications. CO_2 has negligible GWP, is non-flammable, and is environmentally compatible. However, it operates at significantly higher pressures, which requires robust system design and specialized components.

Among the alternative refrigerants under consideration, propane (R290) has emerged as a promising candidate due to its favorable thermodynamic and environmental characteristics. R290 is a natural hydrocarbon refrigerant with a very low global warming potential (GWP = 3) and zero ozone depletion potential, resulting in a low environmental impact. In addition, it exhibits excellent thermodynamic performance, including high latent heat of vaporization and good heat transfer properties, which can enhance system efficiency compared to conventional refrigerants. Also Compared to synthetic refrigerants such as R1234yf, R290 offers lower refrigerant cost due to its natural availability and simpler production process. Its operating pressures are also comparable to those of R134a and R1234yf, allowing the possibility of adapting existing system designs with relatively minor modifications.

However, the widespread adoption of R290 is limited by its high flammability (A3 classification). Therefore, its application in automotive systems requires a thermal management design in which the refrigerant is confined within a closed circuit and does not enter the passenger cabin. By ensuring that the refrigerant remains isolated from the cabin environment, the associated safety risks can be significantly reduced, making R290 a viable and future-oriented alternative for electric vehicle thermal management systems.[14]

2.3 TMS Architectures in Electric Vehicles

TMS in BEV can be categorized based on the different ways the refrigerant and coolant circuits interact with each other as well as the other key subsystems. These configurations plays a key role in determining the efficiency, safety and complexity of the TMS.

In automotive applications, three primary types of TMS architecture are commonly considered for HVAC application:

1. Direct expansion (DX) systems
2. Semi-Secondary loop (SSL) systems
3. Full-Secondary loop (FSL) systems

Each architecture differs in terms of refrigerant distribution, level of integration with coolant loops, and degree of isolation between the refrigerant and the vehicle cabin.

Figure 2.8 illustrates different thermal architecture used in BEV. In Figure 2.8a a direct expansion (DX) thermal management system, the refrigerant directly reaches the cabin HVAC unit for both cooling and heating operations. During cooling mode, the low-temperature refrigerant flows through the cabin evaporator, where it absorbs heat from the cabin air. During heating mode, the high-temperature refrigerant passes through the internal condenser (iCond), transferring heat directly to the cabin air. Since the refrigerant directly circulates through cabin heat exchangers, the DX system provides high thermal efficiency and fast cabin response. However, this configuration distributes refrigerant throughout the cabin HVAC system, which can raise safety concerns when flammable refrigerants such as R290 are used.

Figure 2.8b illustrates Semi-Secondary loop. In a SSL system, refrigerant is used directly only for cabin cooling, while cabin heating is achieved through a secondary coolant loop. During cooling operation, refrigerant flows through the cabin evaporator and directly cools the cabin air, similar to the DX system. However, during heating operation, heat from the refrigerant loop is first transferred to a coolant circuit through a heat exchanger, and the heated coolant is then circulated to the cabin heater core. In this configuration, refrigerant still enters the cabin during cooling mode, but cabin heating is isolated through the coolant loop. The SSL architecture therefore offers a partial reduction in refrigerant exposure while maintaining efficient cooling performance.

Figure 2.8c illustrates a full-secondary loop (FSL) system, the refrigerant remains confined within a closed refrigeration module and does not directly enter the passenger cabin. Both cabin cooling and cabin heating are achieved using coolant loops. During cooling operation, the refrigerant cools the secondary coolant through a chiller, and the cooled coolant is circulated to the cabin cooler core. Similarly, during heating operation, heat from the refrigerant loop is transferred to another coolant loop through water cooled condensor (WCond), which supplies warm coolant to the cabin heater core. As a result, only coolant circulates through the cabin HVAC unit for both heating and cooling functions. This architecture significantly improves safety when using flammable refrigerants such as R290, as the refrigerant remains isolated from the cabin environment.

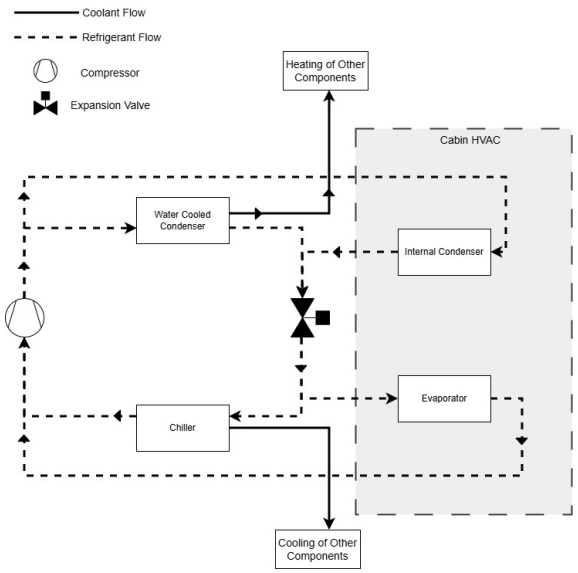

(a) Direct expansion loop

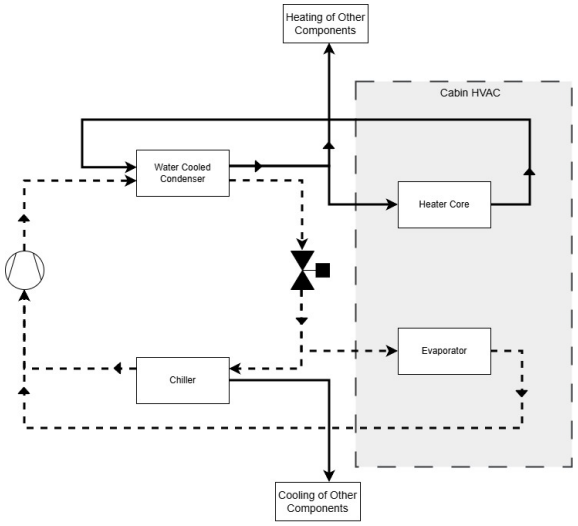

(b) Semi-Secondary loop

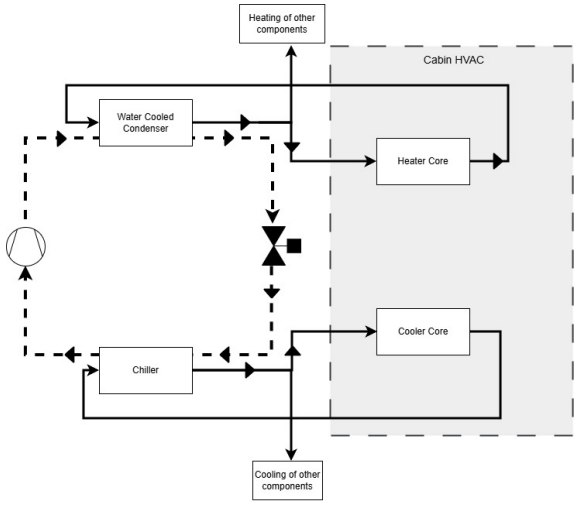

(c) Full-Secondary loop

Figure 2.8: Thermal management system architectures in BEVs

2.4 Research Gap

Recent developments in electric vehicle thermal management systems have increasingly focused on integrated secondary-loop architectures to improve safety, thermal efficiency, and refrigerant management. In particular, FSL systems have gained attention for their ability to isolate the refrigerant from the passenger cabin, making them suitable for the application of flammable low-GWP refrigerants such as R290.[15] Among these developments, Volvo Cars has proposed a FSL TM architecture in which coolant loops are utilized for both cabin cooling and heating, while the refrigerant remains confined within a closed refrigeration module.

Although previous studies have investigated integrated TM architectures and alternative refrigerants, limited research has been conducted on the cooling performance and actuator operating strategies of FSL systems based on the Volvo cars' architecture. In particular, the coordinated operation of coolant pumps, valves, and cooling fans significantly influences coolant flow distribution, heat transfer effectiveness, and overall thermal regulation during cooling operation.

Furthermore, the interaction between refrigerant and secondary coolant loops in R290-based FSL systems requires further investigation to identify effective operating strategies that can improve cooling performance while maintaining safe refrigerant isolation from the passenger cabin. Therefore, there is a need to analyze and evaluate actuator operation strategies for integrated FSL TMS in battery electric vehicles.

3
Methods

3.1 Simulation Environment

3.1.1 CVTM

GT-Suite is a comprehensive software platform for physical modeling and simulation, offering a wide range of libraries that contain premodelled components and operating environments. We can incorporate this tool which significantly reduces development time and associated costs by enabling accurate system response analysis and virtual validation of modeled systems.

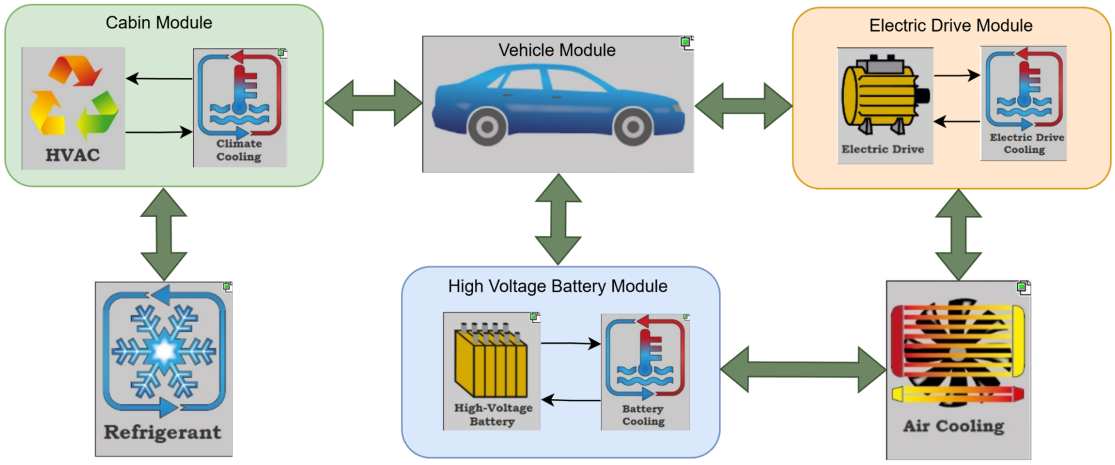

Figure 3.1: CVTM Simulation Environment

At Volvo Cars, a Complete Vehicle Thermal Model (CVTM) has been developed within the GT Suite environment. This simulation platform allows users to evaluate the thermal behavior of the system using 1D model for the complete system, encompassing all subsystems that require heating or cooling. The CVTM plant model includes cabin module, battery module, electric drive module, air cooling as well as the refrigerant and coolant circuits. These systems comprise multi way valves, pipes, pumps, and radiators, whose operation is regulated by control strategies based on heating and cooling demands.

3.2 FSL Architecture

The architecture in Figure 3.2 illustrates the FSL thermal management architecture implemented in the CVTM. The system integrates the refrigerant circuit, cabin HVAC loop, electric drive cooling loop, and battery cooling loop through centralized valve module assemblies for thermal management.

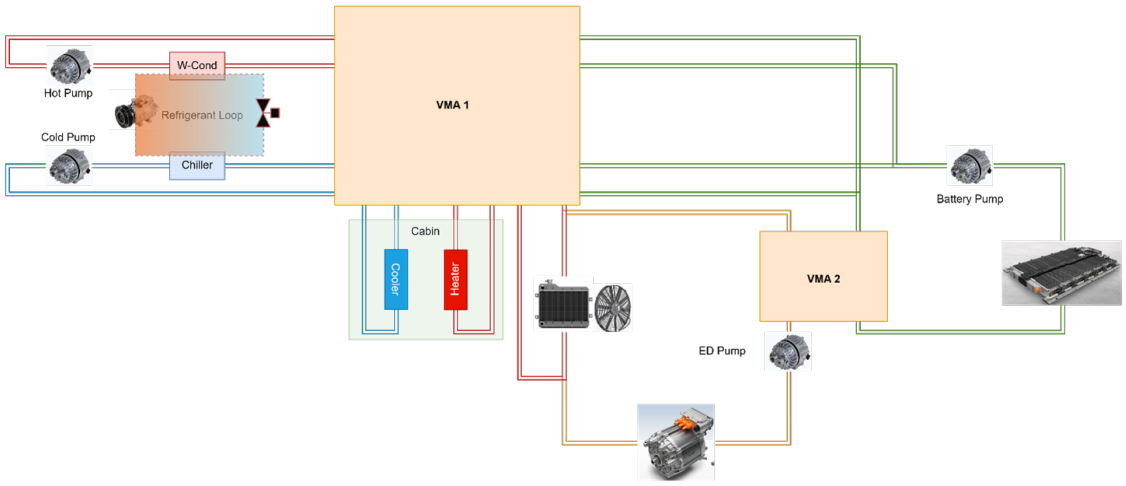

Figure 3.2: FSL Architecture

The cabin consists of the cabin cooler core and heater core. During cooling operation, chilled coolant from the chiller is circulated through the cabin cooler core to extract heat from cabin air. During heating operation, warm coolant is directed from WCond to the heater core to provide cabin heating.

The electric drive cooling loop is connected to the electric motor and power electronics. The coolant circulation through this loop removes heat generated by the electric drive unit during vehicle operation. The thermal energy extracted from the electric drive can either be rejected through the radiator or redistributed within the thermal management system depending on valve operating conditions.

The battery pump circulates coolant through the battery pack to maintain cell temperatures within the desired operating range. Depending on thermal demand, coolant from the battery loop can be routed either toward the chiller for active cooling or toward the radiator for passive heat rejection to the ambient.

The radiator and cooling fan subsystem serve as the primary heat rejection path to the ambient environment. The heat absorbed from the cabin, electric drive, and battery loops is transferred across the refrigerant loop (from chiller to WCond) and rejected to ambient air through forced convection with the help of radiator and cooling fan.

The Valve Module Assemblies (VMA 1 and VMA 2) play a critical role in the system by dynamically controlling coolant flow distribution between the different thermal subsystems. This can be achieved by varying valve proportionality and pump operating conditions, the system can operate in multiple cooling modes including cabin-only cooling, battery-only cooling, electric drive cooling, and combined thermal management modes.

3.3 Modes

The scope of the current thesis is limited to cooling operating modes, namely cabin cooling, battery cooling, and combined cabin–battery cooling. In each mode ED cooling is done passively by rejecting the heat generated in ED circuit to ambient through radiator.

3.3.1 Cabin Cooling Mode

Figure 3.3 illustrates the FSL thermal management architecture configured for cabin cooling operation.

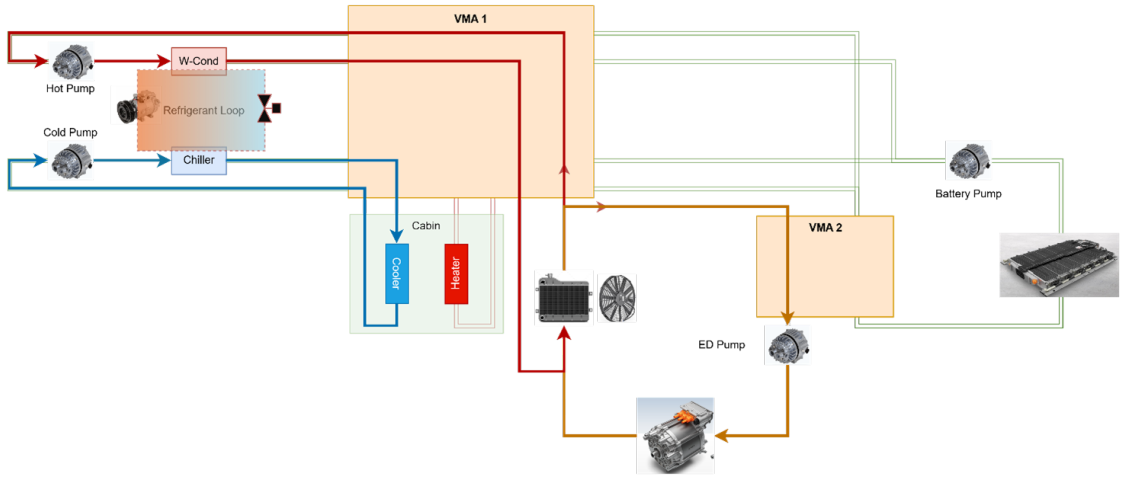

Figure 3.3: Cabin Cooling Mode Layout

In cabin-only cooling mode, the VMA 1 prioritizes coolant flow toward the cabin cooler while minimizing or bypassing coolant flow from chiller to the battery and electric drive cooling circuits. During operation, the cold-side pump circulates coolant through the chiller, where heat is transferred from the coolant to the refrigerant, producing chilled coolant flow. The chilled coolant is then routed through VMA 1 toward the cabin cooler core to extract heat from the cabin air and provide passenger thermal comfort. The absorbed heat from the cabin through coolant loops is transferred to the refrigerant through chiller and it is absorbed by the coolant present in the hot circuit through WCond which is then rejected to the ambient environment through the radiator. This configuration enables thermally decoupled cabin cooling operation.

3.3.2 Battery Cooling Mode

Figure 3.4 illustrates the FSL thermal management architecture configured for battery-only cooling operation.

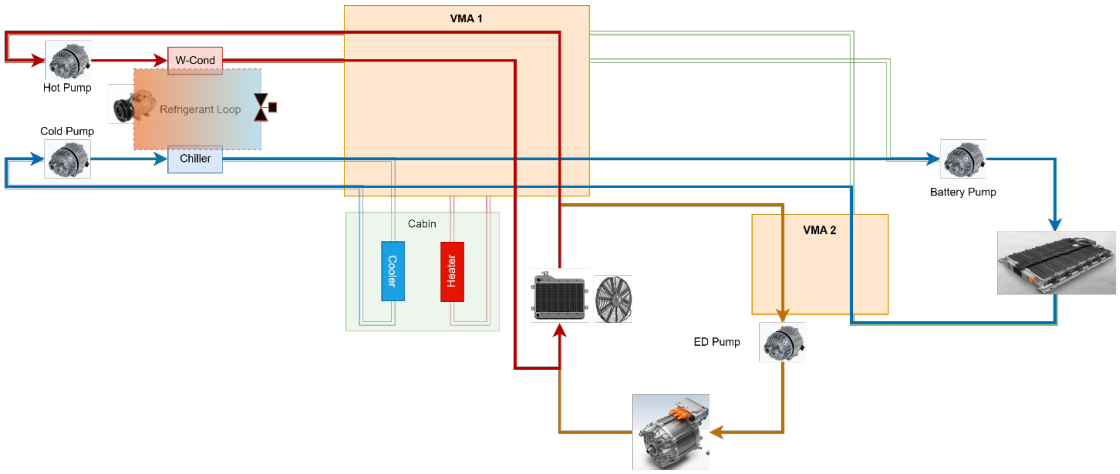

Figure 3.4: Battery Cooling Mode Layout

In this mode, the VMA1 and VMA2 prioritizes coolant flow toward the battery cooling loop while minimizing or bypassing coolant flow from chiller to the cabin and electric drive cooling circuits. During operation, the battery pump circulates coolant through the battery pack, where heat generated due to electrochemical reaction which is absorbed by the coolant. The heated coolant is then routed through the valve module assembly toward the chiller, where heat is transferred from the coolant to the refrigerant loop. The absorbed heat from the refrigerant is subsequently transferred to the hot-side coolant circuit through the WCond and rejected to the ambient environment through the radiator. This configuration enables thermally decoupled battery cooling operation.

3.3.3 Cabin & Battery (Combined) Cooling Mode

Figure 3.5 illustrates the FSL thermal management architecture configured for combined cabin and battery cooling operation. In this mode, VMA1 and VMA2 distribute coolant flow simultaneously toward both the cabin cooling loop and the battery cooling loop based on the thermal demand of each subsystem. During operation, the cold-side pump circulates coolant through the chiller, where heat is transferred from the coolant to the refrigerant, producing chilled coolant flow. The chilled coolant is then routed through VMA1 toward the cabin cooler core to extract heat from the cabin air, while a portion of the coolant is simultaneously directed toward the battery cooling loop to regulate battery temperature.

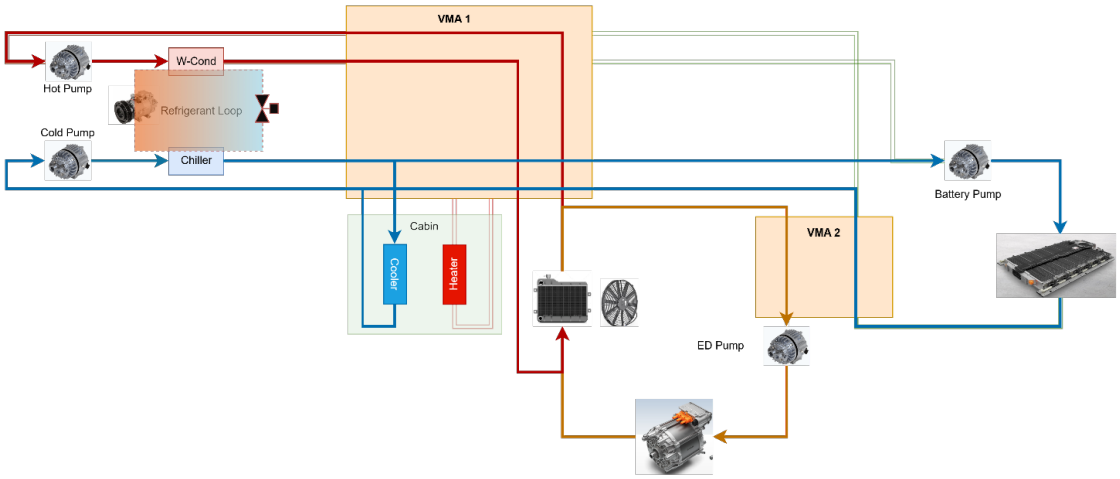

Figure 3.5: Cabin and Battery Cooling Mode Layout

The battery pump circulates coolant through the battery pack, where heat generated is absorbed by the coolant. The absorbed heat from both the cabin and battery coolant loops is transferred to the refrigerant through the chiller and subsequently transferred to the hot-side coolant circuit through the WCond. Finally, the heat is rejected to the ambient environment through the radiator. This configuration enables simultaneous thermal management of passenger cabin comfort and battery thermal stability under combined cooling operating conditions.

The valve assembly module and pump speeds are coordinated rather than independently optimized for a single mode. The valve module assembly dynamically adjusts flow distribution to balance competing thermal needs, ensuring that neither the cabin nor the battery is over or under-cooled. This coordinated control allows dynamic coolant distribution between the cabin and battery cooling loops based on the cooling demand of each subsystem while maintaining system safety and operational robustness.

This mode represents a realistic and frequently encountered operating condition, demonstrating the flexibility of the integrated thermal architecture and its ability to deliver comfort and component protection simultaneously under demanding real-world conditions.

3.4 Simulation Case Studies

The simulation methodology a structured workflow approach developed to evaluate a large number of operating cases efficiently while significantly reducing overall simulation runtime and computational cost. Since full transient thermal simulations require high computational effort, an initial filtering process was introduced to eliminate thermally unsuitable cases at an early stage. Figure 3.6 illustrates the complete simulation workflow adopted in the present study.

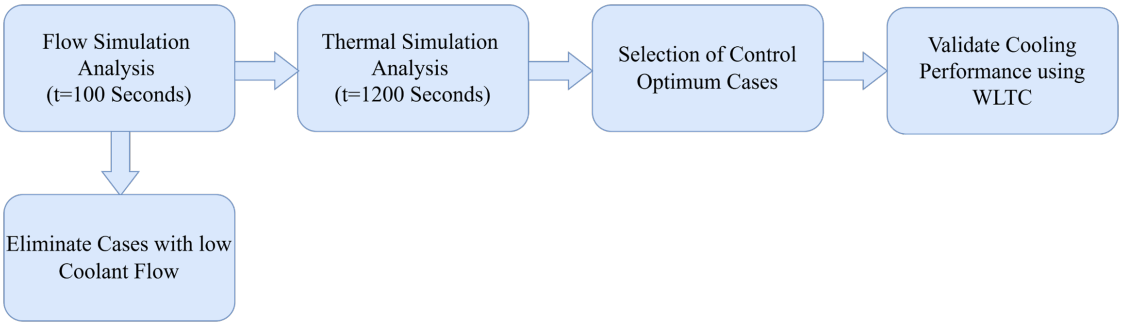

Figure 3.6: Simulation Workflow

The workflow begins with a short-duration flow simulation of 100 seconds, which is primarily intended to evaluate coolant flow distribution within the FSL architecture. At this stage, the objective is not to analyze complete thermal behavior, but rather to verify whether sufficient coolant circulation is achieved across the cabin, battery, electric drive, hot-side, and cold-side cooling loops. Since coolant flow stabilization occurs relatively quickly compared to thermal stabilization, a shorter simulation duration is sufficient to identify cases with inadequate hydraulic performance. This approach considerably reduces computational expense by avoiding unnecessary long-duration thermal simulations.

Following the flow simulations, a flow analysis is carried out to evaluate important parameters such as coolant flow rates (L/min), pump operating behavior, and coolant distribution through the valve module assemblies. Cases exhibiting insufficient coolant flow or operating below the predefined threshold limits are eliminated from further analysis. This filtering process significantly reduces the number of feasible operating conditions and thereby minimizes the total thermal simulation runtime.

The remaining shortlisted cases are subsequently subjected to detailed transient thermal simulations with a duration of 1200 seconds. The extended simulation duration allows the system to capture transient thermal behavior and temperature evolution of the cabin, battery, coolant loops, refrigerant loop, and electric drive system under realistic operating conditions. During this stage, the interaction between coolant flow distribution and heat transfer is evaluated through parameters such as cabin temperature, battery temperature, energy consumption, and COP.

Based on the thermal analysis, the best-performing operating conditions DOE cases are selected considering both thermal performance and energy efficiency. These selected cases are then validated under the Worldwide Harmonized Light Vehicle Test Cycle (WLTC), which introduces realistic transient driving conditions including varying vehicle speed, thermal load fluctuations, and airflow conditions.

The WLTC validation ensures that the developed cooling strategies remain effective, stable, and energy efficient under practical vehicle operating scenarios. Thus, the simulation methodology enables systematic screening of multiple operating conditions while significantly reducing computational time by preventing low-performing cases

from progressing to computationally expensive transient thermal simulations.

3.5 FSL Cooling Strategy Evaluation

This section presents the simulation studies carried out for evaluating the cooling strategies of the FSL thermal management architecture under different operating conditions, as introduced in Section 3.4. The analysis focuses on assessing cooling performance, energy efficiency, and control effectiveness for cabin cooling, battery cooling, and combined cabin–battery cooling modes. The control strategy study investigates the influence of coolant flow distribution, pump operating conditions & valve module assembly proportionality operation on the overall thermal management performance. The simulations are performed under extreme ambient conditions to evaluate transient cooling response, energy consumption, and COP, with the objective of cooling control strategies are evaluated under the specified boundary conditions to analyze their influence on cabin thermal comfort, battery thermal regulation, and overall system energy efficiency.

3.5.1 Parameters Considered for Evaluation

The comparable evaluation is analyzed for the FSL Architecture across all cooling modes by a common set of operating and performance parameters was considered throughout the simulation study. The simulations were performed under an ambient temperature boundary condition of 40°C to represent high ambient thermal conditions encountered during severe vehicle operating scenarios.

The Table 3.1 shown below illustrates operating parameters varied as part of the DOEs which are:

Parameter	Operating Conditions
Pump Duty Cycles	Electric Drive pump, Battery pump, Hot pump, and Cold pump varied between 25%, 50%, 75% & 100% of their maximum operating limits
Fan Speeds	Varied between 0% and 100% of their maximum operating limits
Vehicle Speed	Constant vehicle speeds of 0, 25, 50, 75, and 100 km/h including WLTC operating conditions
Valve Module Assembly Configurations	Different operating configurations of VMA1 and VMA2

Table 3.1: Operating Parameters Considered During DOE Analysis

From the above operating conditions, the performance metrics are extracted from the simulations including coolant flow rates (L/min), cabin and battery temperature profiles, heat energy absorbed (kWh), radiator heat rejection (kWh), total energy

consumption (kWh), and system COP. Cooling time is quantified as the time required to reach the respective target temperature for cabin or battery.

3.5.2 Simulation Boundary Conditions

To ensure consistency and comparability across all DOEs cases, common operating boundary conditions were maintained throughout the study. The simulations were conducted under severe summer operating conditions with an ambient temperature of:

$$T_{amb} = 40°C$$

The selected ambient condition represents a worst-case cooling scenario commonly encountered in hot climatic regions. Under these conditions, the thermal load on the cabin and battery becomes significantly high due to:

- Solar heat gain through windshield and side windows
- Elevated cabin soak temperature
- Increased battery internal heat generation
- Reduced heat rejection effectiveness at high ambient temperatures

The cabin initial temperature was initialized at approximately:

$$T_{cabin\,initial} = 40°C$$

Similarly, the battery initial average temperature was initialized between:

$$T_{battery\,initial} = 35°C - 45°C$$

depending on the operating case.

The target operating temperatures considered during the analysis are:

Subsystem	Target Temperature Range
Cabin	$22°C - 23°C$
Battery	$< 35°C$
Electric Drive Unit	$20°C - 60°C$

Table 3.2: Target Thermal Conditions

3.5.3 Performance Metrics Used for Evaluation

The methodology was developed to investigate the effectiveness of the FSL architecture in achieving:

1. Faster rate of cabin cooling under extreme ambient conditions
2. Faster rate of battery cooling under extreme ambient conditions
3. High COP

4. Lowest Energy consumption
5. Balanced cooling distribution & thermal stabilization during combined cooling operation

3.5.3.1 Cooling Time

Cooling time represents the transient response capability of the thermal management system.
For cabin cooling:

$$t_{cooling\,cabin}$$

is defined as the time required for cabin air temperature to reduce from initial condition to:

$$T_{cabin} \leq 23°C$$

Similarly, for battery cooling:

$$t_{cooling\,battery}$$

is defined as the time required for battery average temperature to reach:

$$T_{battery} \leq 35°C$$

Lower cooling time indicates better transient thermal response.

3.5.3.2 Coefficient of Performance (COP)

The overall thermal efficiency of the system is evaluated using the coefficient of performance.
For Cabin Cooling,

$$COP_{cabin} = \frac{Q_{cabin}}{E_{total}} \tag{3.1}$$

where,

$$Q_{cabin} = \text{Cabin Cooler Heat Energy Absorbed}$$

$$E_{total} = \text{Total Energy Consumed}$$

For Battery Cooling,

$$COP_{battery} = \frac{Q_{battery}}{E_{total}} \tag{3.2}$$

where,

$$Q_{battery} = \text{Battery Heat Energy Absorbed}$$

$$E_{total} = \text{Total Energy Consumed}$$

For Cabin - Battery Combined Cooling,

$$COP_{combined} = \frac{Q_{cabin} + Q_{battery}}{E_{total}} \tag{3.3}$$

where,

$$Q_{cabin} = \text{Heat Absorbed in Cabin}$$
$$Q_{battery} = \text{Heat Absorbed in Battery}$$
$$E_{total} = \text{Total Energy Consumed}$$

Higher COP indicates that energy consumed by auxiliary unit in thermal system is properly utilized to reject heat from respective component.

3.5.3.3 Energy Consumption

The energy consumption of each operating mode was evaluated using integrated power consumption over simulation duration. The total auxiliary energy consumption is:

$$\begin{aligned} E_{total} = {} & E_{Radiator\,cooling\,fan} + E_{Cabin\,blower\,fan} + E_{Battery\,Pump} \\ & + E_{Electric\,drive\,Pump} + E_{Hot\,Pump} + E_{Cold\,Pump} \\ & + E_{Compressor} \end{aligned} \tag{3.4}$$

The objective is to minimize total energy while maintaining acceptable thermal performance.

3.5.4 Cabin Cooling Mode Strategy

The cabin cooling mode illustrated in Figure 3.3 represents operating conditions where passenger thermal comfort becomes the dominant cooling requirement.

During this operating mode:

- Battery cooling loop remains isolated
- Cabin receives chilled coolant flow
- Valve module prioritizes cabin cooling path
- Compressor operates according to cabin thermal load

The cabin-only cooling analysis was divided into two major objectives.

3.5.4.1 Cabin Cooling Strategy 1: Faster Cabin Pull-Down

The primary objective of this strategy is to reduce cabin air temperature as quickly as possible.

Under high ambient conditions, cabin temperature increases rapidly due to:

- Solar radiation load
- Conduction heat transfer from body panels

- Occupant heat generation
- High ventilation thermal load

To investigate rapid cabin cooling behavior the following parameters are evaluated to analyze their effect on overall thermal system:

- Cold pump speed
- Hot pump speed
- Electric drive pump speed
- Chiller coolant outlet temperature
- Ambient temperatures

3.5.4.2 Cabin Cooling Strategy 2: High COP and Low Energy Consumption

The second strategy focuses on energy-efficient cabin cooling by evaluating operating conditions as below:

- Stable cabin cooling
- Lower pump energy consumption
- Variation in system COP

The different cold pump operating conditions are evaluated to analyze their influence on:

- Compressor operating behavior
- Energy consumption
- Overall thermal system efficiency

The influence of pump operating conditions on cabin cooling performance and energy consumption is being investigated throughout the simulations.

3.5.5 Battery Cooling Mode Strategy

The battery only cooling operation becomes dominant during:

- High discharge loads
- Fast charging conditions
- High ambient operation
- Continuous uphill or aggressive driving

The battery thermal management objective differs from cabin cooling because lithium-ion batteries require:

- Stable thermal gradients
- Controlled cooling rate
- Uniform temperature distribution

3.5.5.1 Battery Cooling Strategy 1: Faster Battery Cooling

This strategy focuses on investigating aggressive heat extraction from the battery loop.

The following operating conditions is evaluated during the simulations to analyze their effect on overall thermal system:

- Battery pump speed
- Cold pump speed
- Electric drive pump speed
- Radiator fan speed at different vehicle speed

Battery heat generation is generally evaluated using the internal resistance relationship:

$$Q_{battery} = I^2 R \tag{3.5}$$

where:

- $Q_{battery}$ = battery heat generation
- I = battery current
- R = internal resistance

The thermal response of the battery cooling loop was analyzed using:

- Battery average temperature
- Maximum cell temperature
- Temperature spread ΔT
- Cooling rate

3.5.5.2 Battery Cooling Strategy 2: High COP Low Energy Cooling

This operating strategy focuses on energy-efficient battery cooling by analyzing:

- Energy consumption
- Battery thermal stability
- Overall thermal system efficiency (COP)

3.5.6 Combined Cabin and Battery Cooling Mode Strategy

Combined cooling mode represents realistic electric vehicle operating conditions where both cabin cooling demand and battery cooling demand exist simultaneously. In this operating mode:

- Cabin cooling demand exists simultaneously
- Battery cooling demand becomes active
- Cooling capacity is distributed dynamically between thermal loops

The valve module assembly plays an important role in controlling proportional coolant distribution between cabin and battery loops.

3.5.6.1 Combined Cooling Strategy 1: Energy efficient Combined Cooling

This strategy focuses on evaluating balanced cooling operation with reduced energy consumption.

The operating conditions were adjusted to investigate:
- Balanced coolant distribution
- Compressor cycling behavior
- Pump operating conditions
- Thermal stability
- System COP study

3.5.6.2 Combined Cooling Strategy 2: Prioritized Cabin Cooling with Battery Cooling

This strategy prioritizes passenger thermal comfort during the initial transient phase.

Initially:
- Higher coolant flow was directed toward the cabin loop
- Reduced coolant flow was supplied to the battery loop
- Cabin thermal response was monitored

After cabin temperature stabilization:
- Additional cooling capacity was redistributed
- Battery cooling flow conditions were adjusted

This strategy was evaluated based on:
- Cabin cooling response
- Battery thermal state
- Compressor operating behavior
- Coolant flow redistribution

3.5.6.3 Combined Cooling Strategy 3: Prioritized Battery Cooling with Cabin Cooling

This strategy is considered for operating conditions where battery thermal control becomes the main priority while cabin cooling is still required. Such a situation can occur during fast charging, where the battery may generate significant heat due to high charging current. If passengers remain inside the vehicle during charging, cabin cooling is also needed to maintain comfort. Therefore, the thermal management system must support both battery cooling and cabin cooling at the same time, but with higher priority given to battery temperature reduction.

During this mode initially more coolant flow is directed towards the battery loop till the battery reaches safe operating temperature when

$$T_{battery} = 40°C$$

The valve proportionality is changed depending upon the requirements

The system operating conditions were modified through:
- Valve assembly module proportionality variation
- Battery pump speed variation

3.5.7 WLTC Validation Methodology

The final shortlisted operating conditions were evaluated using the Worldwide Harmonized Light Vehicle Test Cycle (WLTC).

WLTC introduces dynamic vehicle speeds with variable airflow conditions as per realistic transient operating behavior.

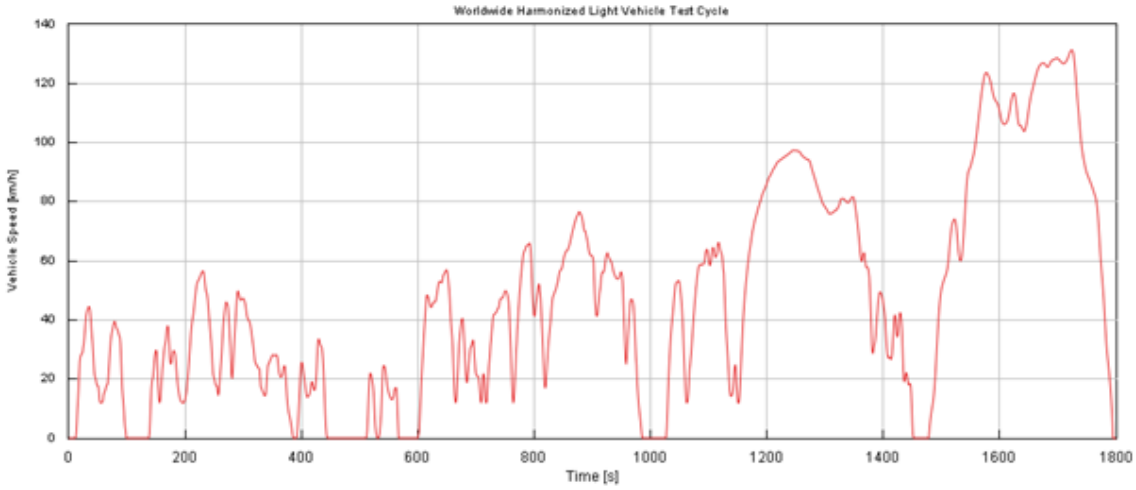

Figure 3.7: Worldwide harmonised Light vehicles Test Cycle (WLTC)

The WLTC simulations were used to evaluate the effectiveness of the developed cooling strategies under realistic transient operating conditions.

The following parameters were monitored throughout the WLTC cycle:
- Cabin temperature
- Battery average temperature
- Auxiliary energy consumption
- System COP

4

Results

This section presents the simulation results for cabin cooling, battery cooling, and combined cabin–battery cooling modes. The analysis focuses on coolant flow distribution, thermal response, energy consumption, and coefficient of performance under different actuator operating conditions. Based on the results, suitable cooling control strategies are identified to improve cooling response and energy efficiency under high ambient temperature conditions.

4.1 Cabin Cooling Results

Figure A.1 in Appendix shows the coolant flow distribution during cabin cooling mode for different operating cases. Cases in which the flow rate in any pump falls below the defined threshold are removed from the analysis, and only the remaining feasible cases are selected for detailed thermal analysis (shown in green in table [A.1]). The cold-side pump directly affects cabin cooling by circulating chilled coolant from the chiller to the cabin cooler core. Higher cold-side flow improves heat removal from the cabin and can reduce pull-down time. The hot-side pump controls heat rejection through the water-cooled condenser and radiator loop. Improved heat rejection reduces the load on the refrigerant circuit, allowing the compressor to operate with lower power demand. The electric drive coolant flow is also influenced by the hot-side loop because both circuits are hydraulically connected through the radiator side.

Figure 4.1 shows the feasible ED pump and hot-side pump speed combinations that satisfy this requirement. Since both the ED circuit and hot-side circuit can supply coolant to the radiator, the final flow distribution depends on the combined operation of both pumps. Some combinations may cause hydraulic dominance, where one loop restricts the flow contribution of the other. Therefore, only balanced operating points with sufficient flow in both circuits are selected for further cooling performance analysis.

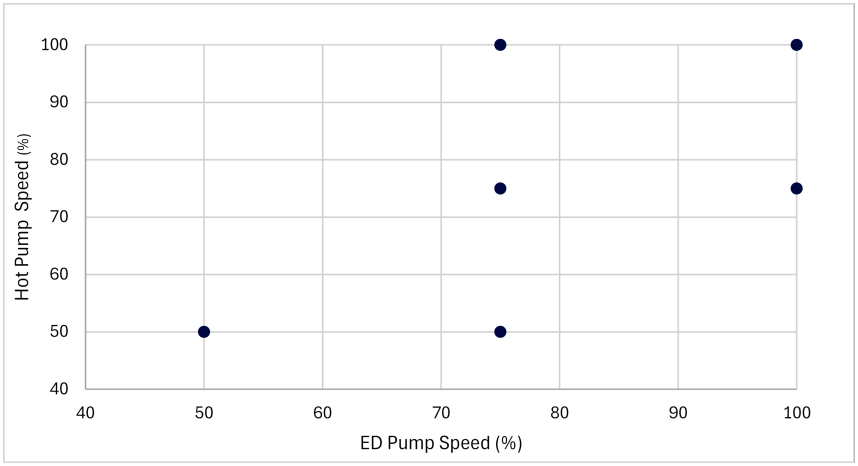

Figure 4.1: Feasible ED pump and hot-side pump speed combinations satisfying the minimum coolant flow criterion.

4.1.1 Cabin Cooling Strategy Results for Faster Cabin Pull Down

The coolant flow from the chiller to the cabin cooler core has a direct influence on cabin cooling performance. Figure 4.2 illustrates that when the cold pump is operated at higher speed, a larger amount of chilled coolant is supplied to the cabin cooler core, improving the heat transfer between the cabin air and the coolant. This enhances heat removal from the cabin and results in a faster reduction in cabin temperature.

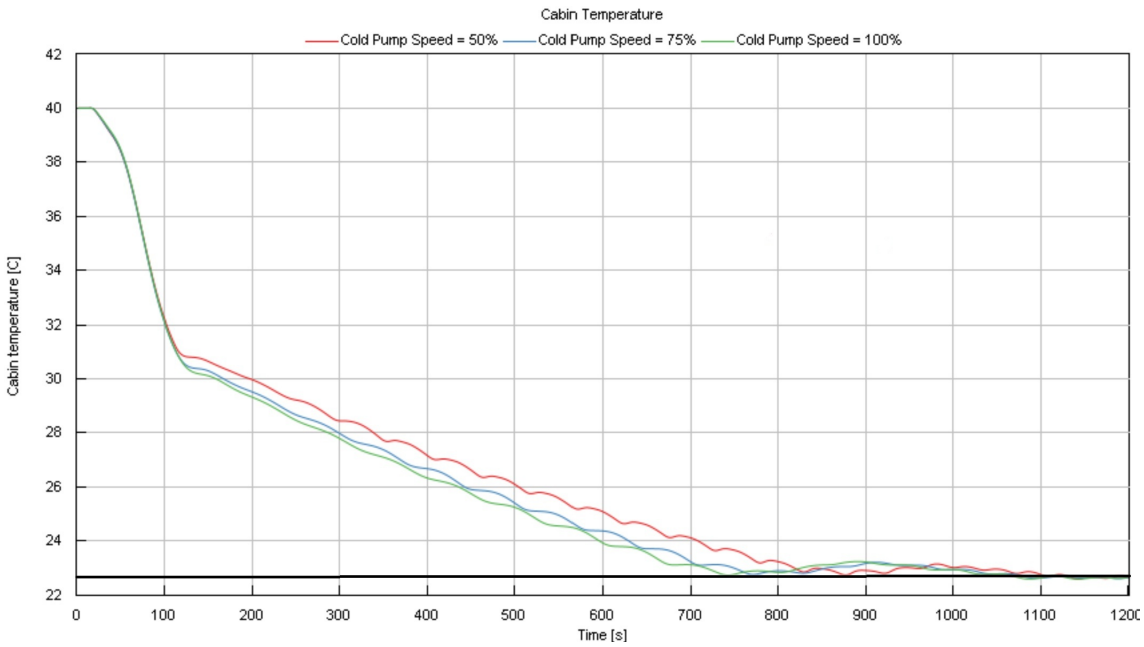

Figure 4.2: Cabin temperature pull-down response at different coolant pump speeds.

Figure 4.3 shows the effect of coolant flow rate through the cabin cooler on the time and energy required to reach the target cabin temperature of 23°C. Time taken and energy consumed are presented in normalized form with respect to the reference case. Therefore, the value of 100 does not represent 100 s or 100 Wh; instead, it represents the reference value used for comparison. The results show the relative change in cooling time and energy consumption as the cold pump speed is varied.

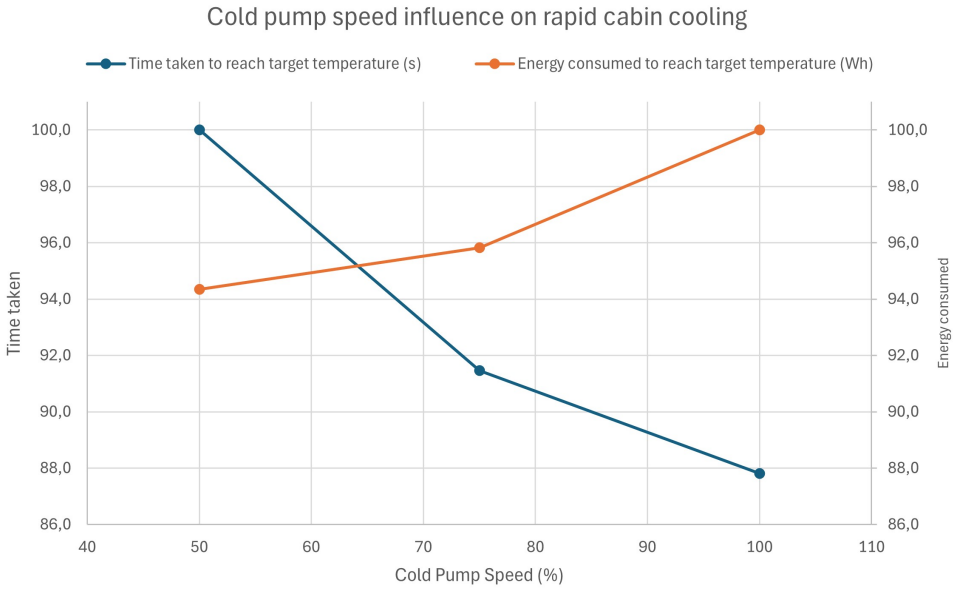

Figure 4.3: Time taken and energy consumed by the TMS system to reach the target temperature at different cold pump speed

As the coolant flow rate increases, the time required to cool the cabin decreases. However, the energy consumed to reach 23°C increases with higher coolant flow. This is mainly due to the higher actuator power demand, especially from the coolant pump and associated cooling components. Therefore, although increasing coolant flow improves cabin pull-down performance, it also leads to greater energy consumption.

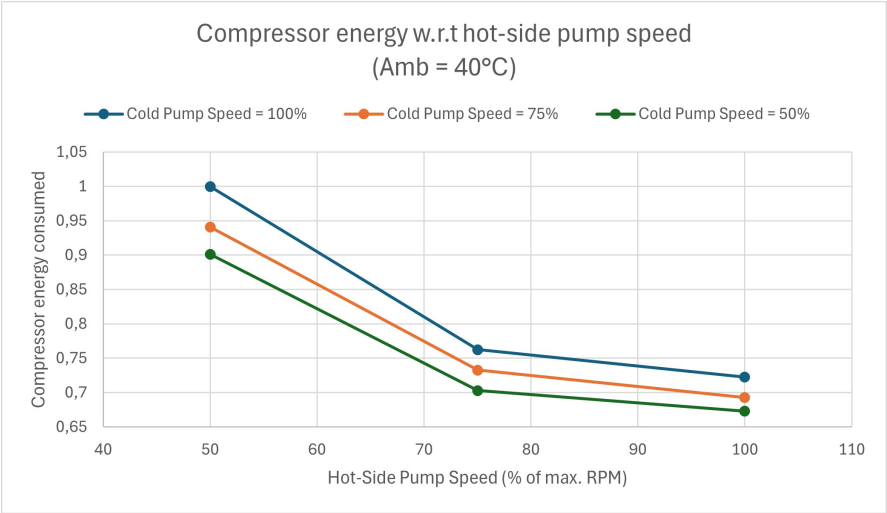

(a) Effect of hot-side pump speed on compressor energy consumption

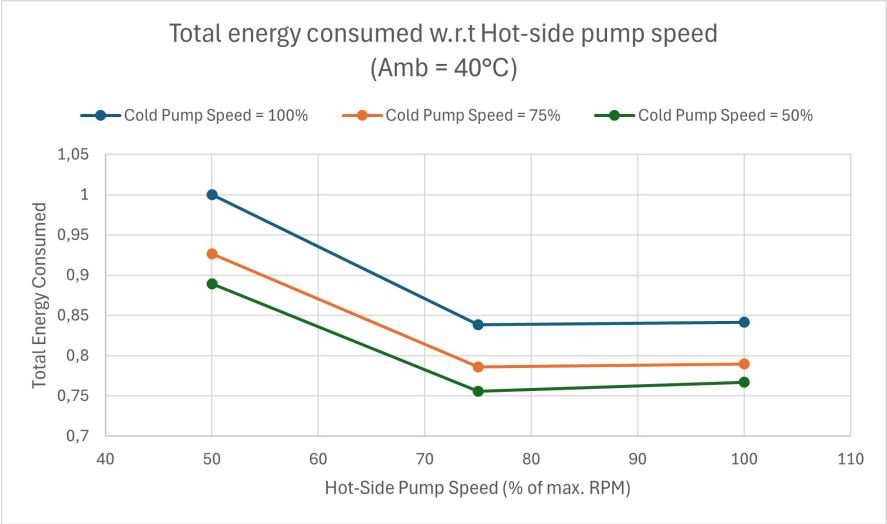

(b) Effect of hot-side pump speed on total energy consumption

Figure 4.4: Effect of WCond pump operation on TMS energy consumption

The results in 4.3 show a clear trade-off between cabin pull-down time and energy consumption. Although the 100% cold pump speed provides the fastest cooling response, it also results in the highest energy consumption. In contrast, the 50% pump speed consumes less energy but requires a longer time to reach the target cabin temperature. Therefore, 75% cold pump speed is selected as the preferred operating condition because it provides a good balance between cooling performance and energy efficiency. This operating point significantly reduces the pull-down time compared to 50% pump speed, while avoiding the additional energy penalty associated with 100% pump operation.

As illustrated in Figure 4.4 at 40°C ambient temperature, very low hot-side pump speed is not suitable because it limits heat rejection and increases compressor energy consumption. Based on the trade-off between compressor energy reduction and total

system energy, 75% hot-side pump speed can be considered an effective operating point for cabin cooling.

4.1.2 Cabin Cooling Strategy Results for High COP and Low Energy Consumption

In section 4.1.1 we evaluated actuator settings for faster cabin pull-down. The results showed that increasing cold-side pump speed improves the cabin cooling response, while higher WCond pump speed improves heat rejection and reduces compressor workload. However, operating the pumps at higher speeds also increases auxiliary energy consumption. Therefore, this section evaluates the energy-efficient cooling strategy, where the objective is to maintain acceptable cabin cooling while reducing total energy consumption and improving COP.

Figure 4.5 shows the comparison of energy consumption for the selected WLTC cases at 40°C ambient temperature. From the 18 feasible cases obtained after the flow survey, four cases were selected based on their energy-efficient cooling performance from the 1200 seconds thermal simulation (Case 1-4). These selected cases were then evaluated under the WLTC driving cycle and compared with a random case (Case 5) and the reference case, where all pumps are operated at maximum speed (Case 6).

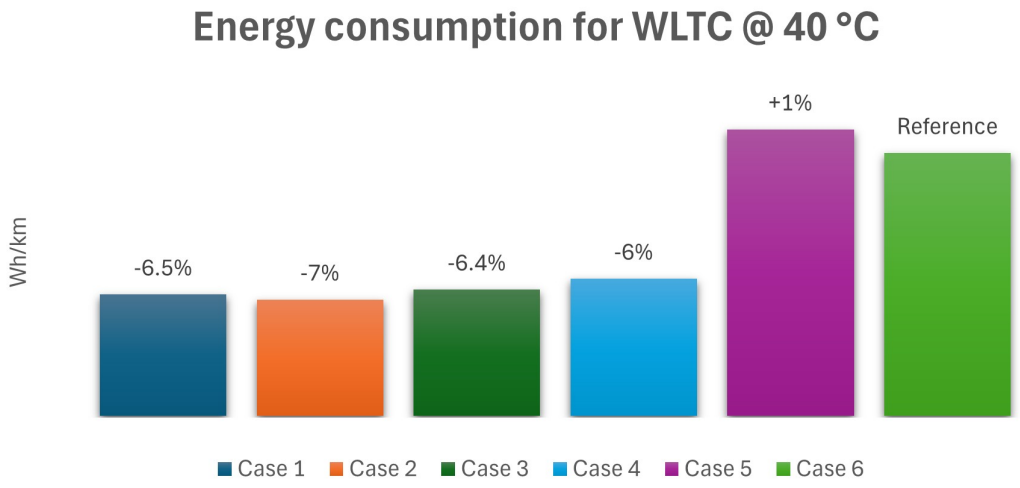

Figure 4.5: Energy consumption comparison of selected WLTC cabin cooling cases at 40°C ambient temperature.

The results show that selected most efficient pump-speed combinations can lower the energy consumption by 7% compared with full pump operation while maintaining acceptable cabin cooling performance. But also we can observe from Figure 4.2 that since the cold-pump is operating at 50% speed in the most efficient case, the cooling time would be slightly higher. Hence we should make a tradeoff strategy of when to use Fast Cabin Cooling and when we should implement Efficient Cabin Cooling strategy.

Table 4.1: Selected operating cases for WLTC energy comparison at 40°C ambient temperature

Case	Cold Pump (%)	ED Pump (%)	Hot-side Pump (%)	Description
Case 1	50	50	50	Selected energy-efficient case
Case 2	50	75	75	Best energy-saving case
Case 3	50	75	100	Selected energy-efficient case
Case 4	75	75	75	Selected energy-efficient case
Case 5	100	75	50	Selected random case
Case 6	100	100	100	Reference: all pumps at maximum speed

Table 4.2: Proposed two-stage cabin cooling strategy

When Used	Cold Pump (%)	ED Pump (%)	Hot-side Pump (%)	Purpose
Initial cooling stage, $T_{cabin} > T_{target} + 2$	75	75	75	Fast cabin temperature reduction
After cabin reaches target temperature	50	75	75	Efficient cooling

Another factor which effect the overall TMS efficiency is the radiator cooling fan speed. During cabin cooling, heat rejected from the coolant coming out of WCond is rejected through radiator to the ambient. Figure 4.6 shows that at lower vehicle speeds, the ram-air effect is limited, hence the radiator cooling fan should operate at higher speed to reject heat from coolant flowing through the radiator to the ambient. On the other hand, when the vehicle speed is higher, natural airflow coming through the shutters helps to reject heat from the radiator. During high vehicle speed, fan speed does not significantly help to release heat, instead if we run the fan, it will add to more auxillary power consumption. The cases used for the analysis are the 4 energy efficient cases used in the previous section (Case 1-4).

In Figure 4.6a we can see at vehicle speed 0 km/h, there is no ram-air flow through the radiator. Therefore, low fan speeds are not sufficient to reject heat effectively, resulting in lower COP. As the fan speed increases, heat rejection improves and COP rises significantly. The maximum COP is obtained around 75% fan speed, after which further increase in fan speed slightly reduces COP due to additional fan power consumption but no improvement in heat rejection through radiator.

The COP values shown in Figure 4.6 are calculated using the formula:

$$COP = \frac{Q_{\text{rad}}}{E_{\text{total}}} \tag{4.1}$$

where Q_{rad} represents the heat rejected through the radiator, and E_{total} represents the total energy consumed by the compressor, pumps, and radiator fan.

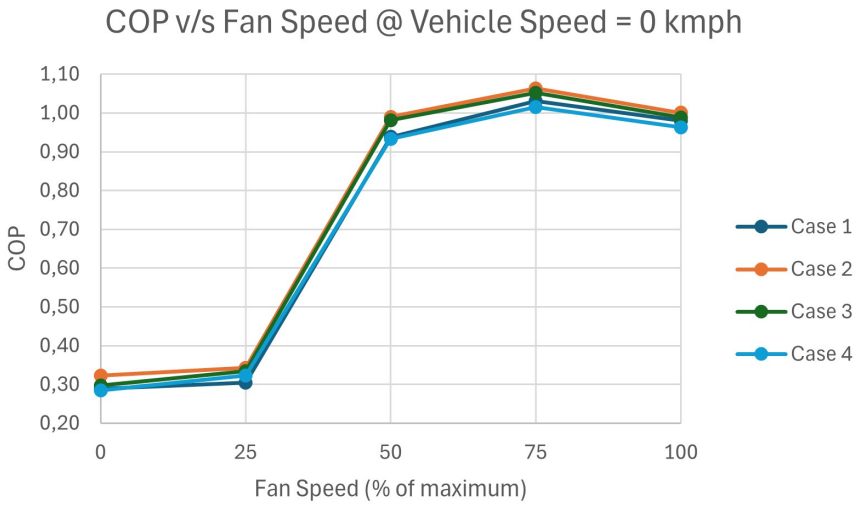

(a) COP variation with fan speed at 0 km/h vehicle speed

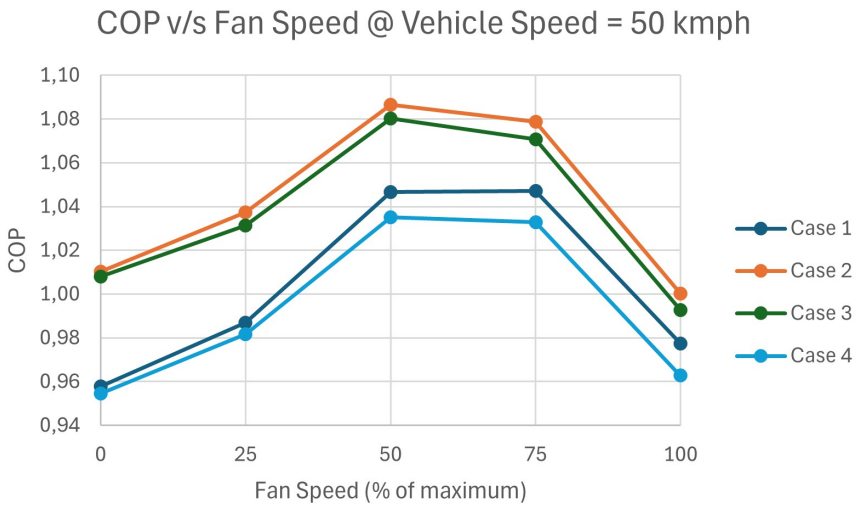

(b) COP variation with fan speed at 50 km/h vehicle speed

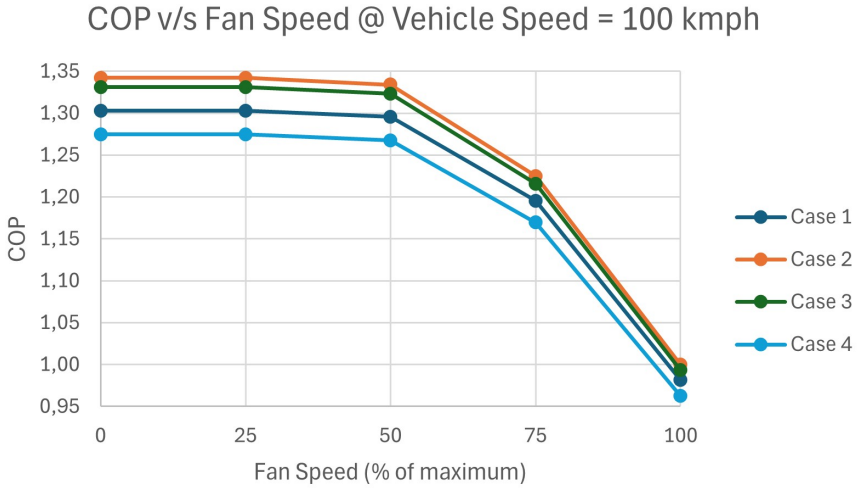

(c) COP variation with fan speed at 100 km/h vehicle speed

Figure 4.6: Effect of radiator fan speed on COP at different vehicle speeds during cabin cooling operation.

Similarly at 50 km/h as shown in Figue 4.6b, some natural airflow is already available due to vehicle motion. Therefore, the system does not require very high fan speed to maintain heat rejection. The COP reaches its maximum around 50% fan speed, showing that moderate fan operation is sufficient at medium vehicle speed.

At 100 km/h, the ram-air effect is strong, and the radiator receives sufficient airflow from vehicle motion. In this case, the highest COP is observed at low or zero fan speed. Increasing fan speed reduces COP because the fan consumes additional power while providing little improvement in heat rejection. Therefore, fan operation should be minimized at high vehicle speeds.

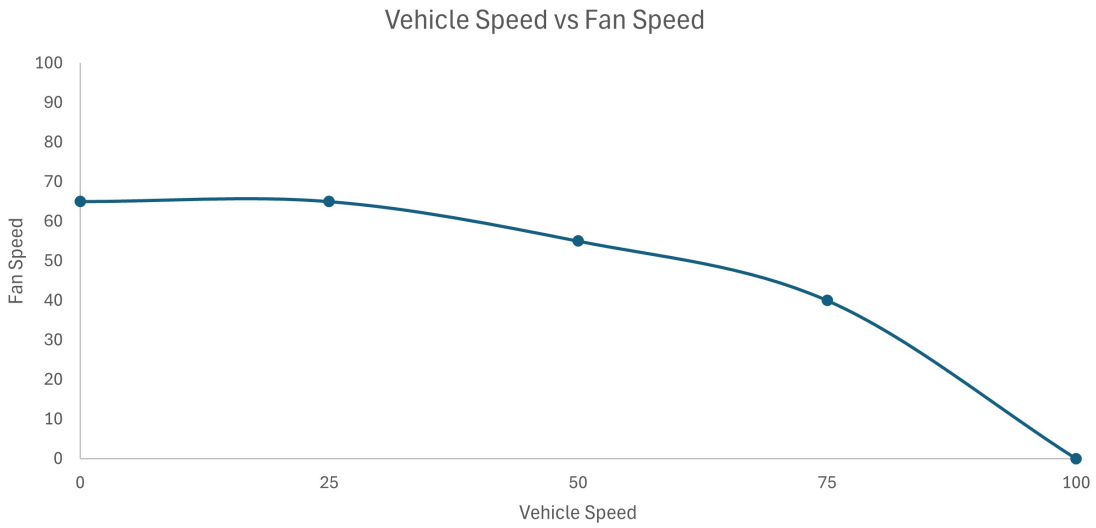

Figure 4.7: Optimized fan speed map with respect to vehicle speed for cabin cooling mode.

Based on the COP variation observed at different vehicle speeds, the vehicle-speed-based fan speed map was developed as shown in Figure 4.7. The map assigns higher fan speed at low vehicle speeds, where ram-air cooling is limited, and gradually reduces fan speed as vehicle speed increases. This fan speed map is then used for the WLTC simulation to improve system efficiency while maintaining sufficient radiator heat rejection.

Figure 4.8 shows the radiator fan command applied over the WLTC cycle based on the optimized vehicle-speed-dependent fan map. The red curve represents the WLTC vehicle speed profile, while the blue curve shows the corresponding fan speed command.

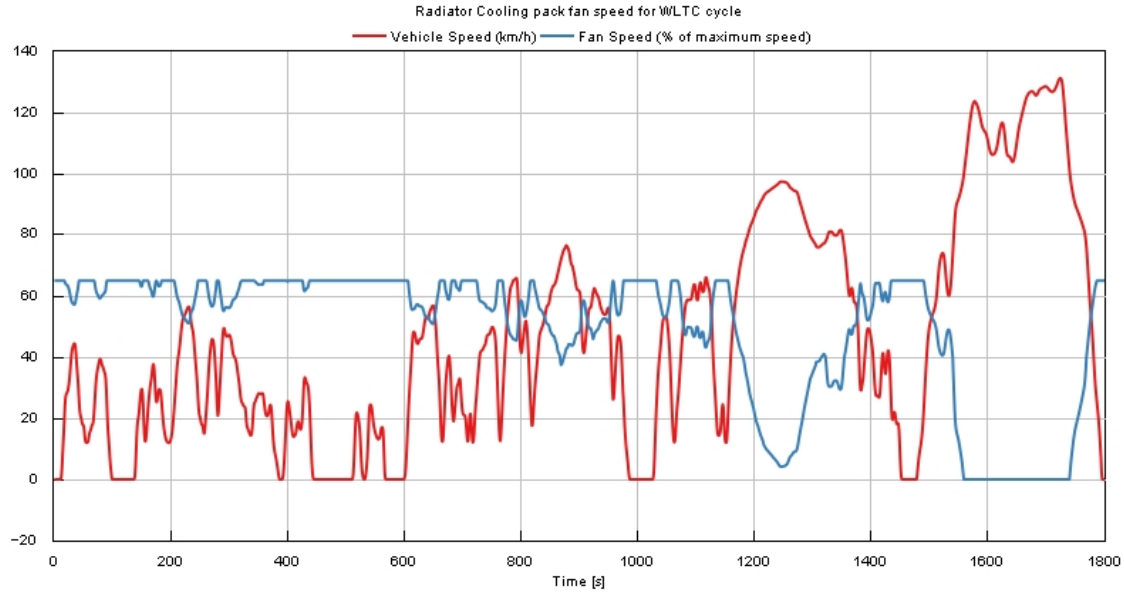

Figure 4.8: Controlled radiator fan speed for WLTC cycle during cabin cooling mode.

As illustrated in Figure 4.10 compared to the full-actuation reference case (all pumps and radiator cooling fan running at 100% speed), the proposed control strategy, as mentioned in Table 4.2 and using the optimized fan speed map, the total battery energy consumption can be reduced by approximately 4.25% during the WLTC drive cycle (23.18 km), while maintaining similar cabin comfort conditions as the full-actuation referance case provides (Figure 4.9). Assuming similar cabin cooling operating conditions, the observed energy reduction could correspond to an approximate range improvement of 21 km for a vehicle with a nominal 500 km range.

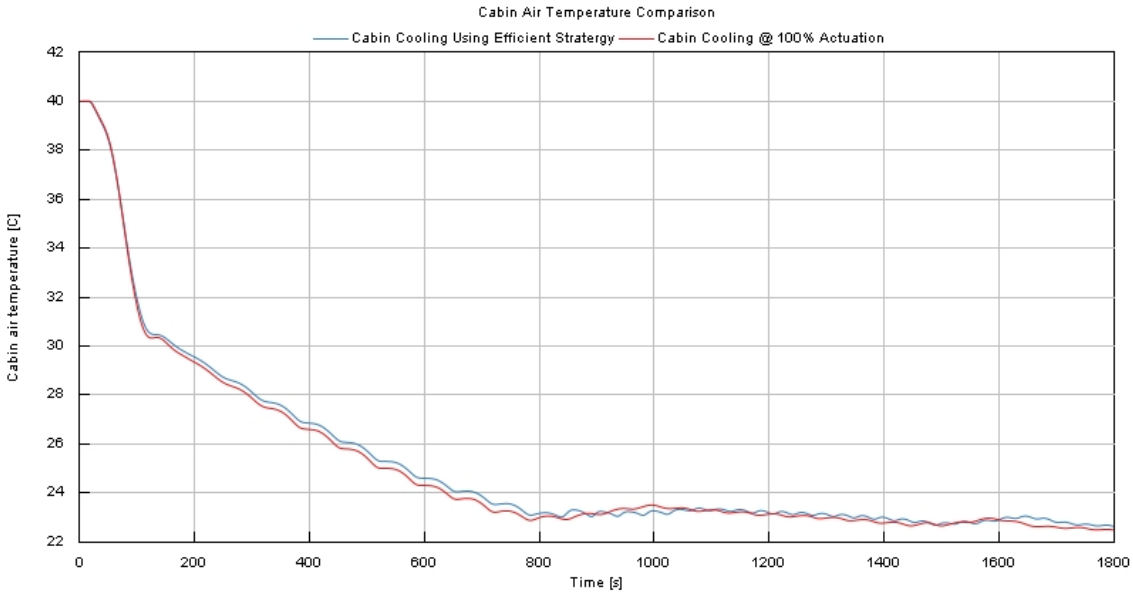

Figure 4.9: Cabin temperature comparison for 100% actuation and efficient control strategy.

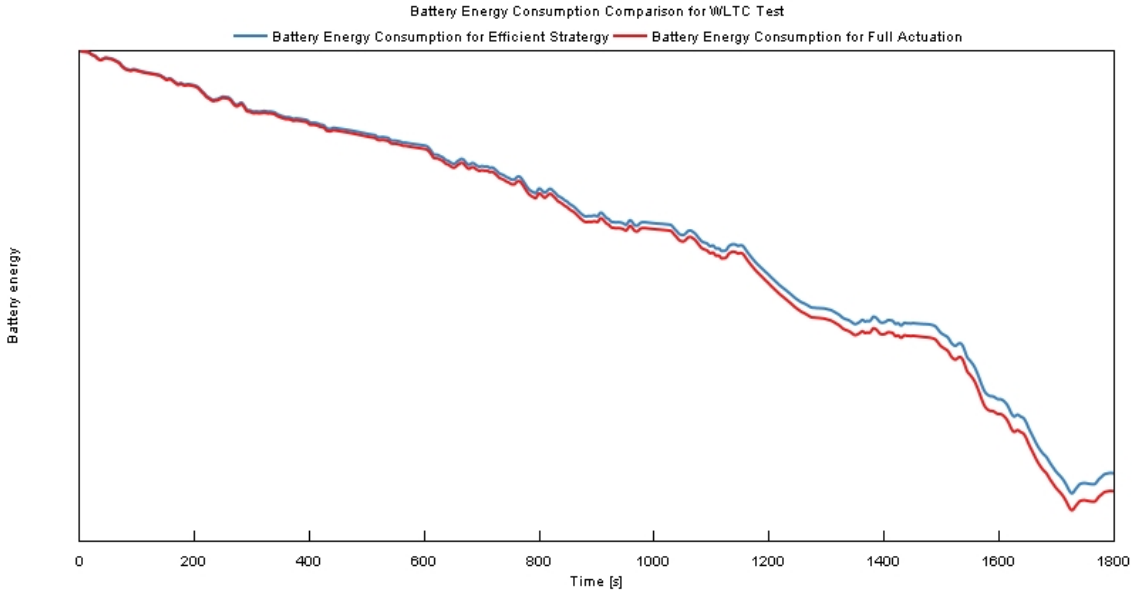

Figure 4.10: Battery energy consumption comparison between the efficient strategy and full-actuation strategy for cabin cooling during the WLTC test.

4.2 Battery Cooling Results

4.2.1 Battery Cooling Strategy Results for Faster Battery Pull Down

Figure 4.11 illustrates the battery temperature variation with time for different cold and battery pump speed combinations during the faster battery pull-down process. In all cases, the battery temperature decreases continuously from an initial temperature of 45°C, demonstrating the effectiveness of the cooling system. The rapid reduction of battery temperature is essential in battery thermal management systems to prevent overheating, maintain battery safety, and improve overall battery performance during high thermal load conditions. Therefore, for the faster battery pull-down strategy, different cold and battery pump speed combinations are investigated to evaluate their influence on battery cooling performance in battery cooling mode operation.

The objective of this analysis is to reduce the battery temperature from 45°C to the target temperature of 35°C as quickly as possible while also analyzing the corresponding cooling time and total energy consumption. In this FSL layout, the cold pump and battery pump play a significant role in controlling coolant circulation and heat rejection, directly influencing the battery thermal pull-down rate, cooling efficiency, and overall energy usage of the thermal management system.

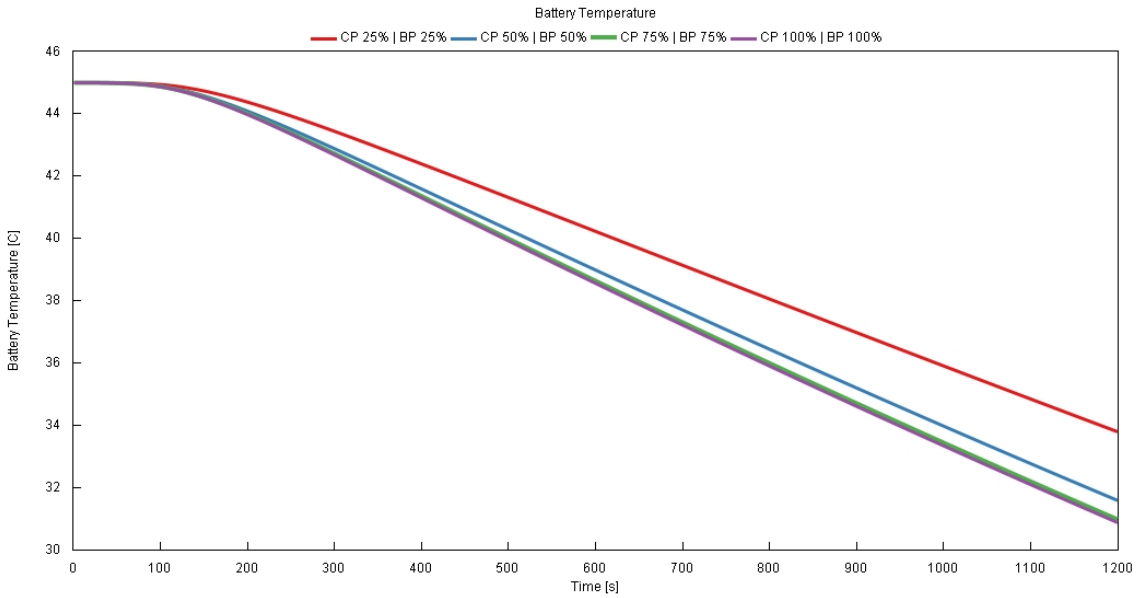

Figure 4.11: Battery cooling faster pull down test result

Figure 4.11 highlights the influence of maintaining equal cold and battery pump speeds on battery thermal management performance. When both pumps operate at the same speed, the coolant circulation and heat exchange become more balanced, resulting in smoother and more effective heat removal from the battery pack. Increasing the pump speeds simultaneously from 25% to 75% greatly enhances cooling efficiency, while the improvement from 75% to 100% is relatively small. This indicates that diverting the maximum coolant flow to the chiller and providing lower coolant flow for electric drive system can achieve the cooling performance. Therefore, maintaining balanced cold and battery pump speeds provides stable thermal control and faster rate of battery cooling performance. The detailed comparison of the cooling time required to reach 35°C and the corresponding target temperature to be achieved is presented in Table 4.3.

Cold Pump Speed (%)	**Battery Pump Speed (%)**	**Time to Reach 35°C (min)**
25	25	19.0
50	50	17.0
75	75	15.7
100	100	15.5

Table 4.3: Cooling Time for Different Pump Speed Combinations

Table 4.3 presents the cooling time required for the battery temperature to decrease from 45°C to 35°C. The results show that increasing both pump speeds improves the battery cooling performance by reducing the pull-down time. At 25% pump speed, the battery requires approximately 19 minutes to reach 35°C, whereas at

100% pump speed the cooling time decreases to about 15.5 minutes. However, the reduction in cooling time becomes smaller at higher pump speeds, particularly between the 75% and 100% cases. Although the maximum pump speed provides the fastest cooling but the improvement is small as compared to the CP 75% & BP 75% case but there is 6.3% additional energy required when compared to 100%. This indicates this combination can be considered an effective compromise between faster rate of cooling and energy efficiency which can be witnessed in Figure 4.8.

The percentage increase in total energy consumption is calculated by normalizing each pump speed case with respect to the baseline CP 25% | BP 25% condition using:

$$\% \text{ Increase} = \frac{E_i - E_{25\%}}{E_{25\%}} \times 100 \tag{4.2}$$

where E_i represents the total energy consumption at a given pump speed combination and $E_{25\%}$ represents the energy consumption of the reference CP 25% | BP 25% case. This normalization method allows the relative increase in energy demand at higher pump speeds to be compared with respect to the minimum energy consumption condition.

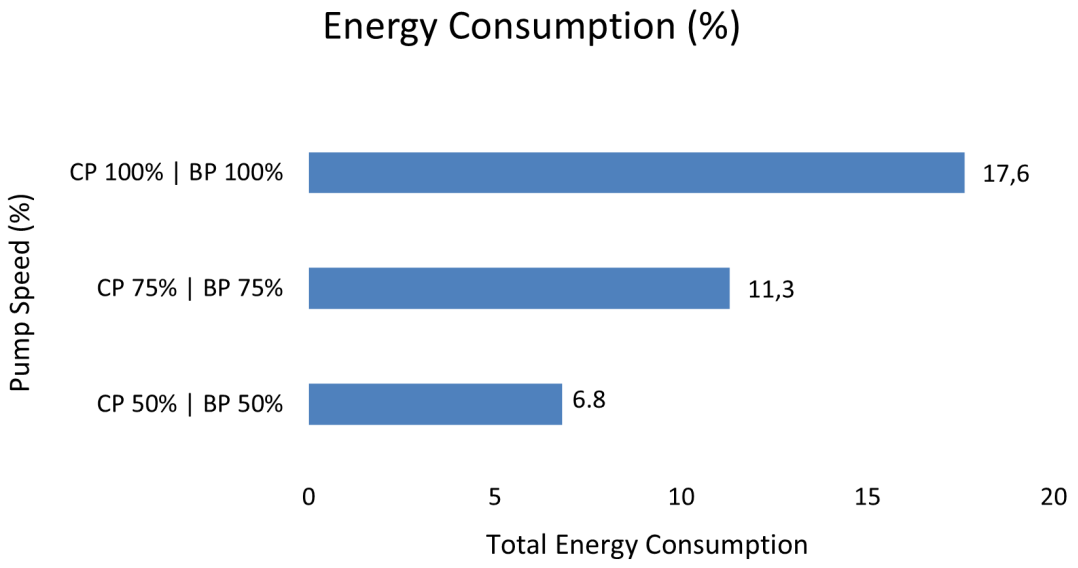

Figure 4.12: Energy consumption comparison for cold-pump speed and hot-pump speed during battery cooling mode.

Figure 4.12 illustrates the normalized increase in total energy consumption for different cold pump (CP) and battery pump (BP) speed combinations. The graph clearly shows that increasing both pump speeds results in a progressive rise in

energy consumption due to the higher coolant circulation flow rate. As the pump speed increases from 50% to 100%, the percentage increase in energy consumption becomes significantly larger, indicating that the thermal management system requires substantially more energy to sustain higher coolant flow rates.

The graph also highlights the trade-off between cooling performance and system efficiency. Although higher pump speeds improve the battery thermal pull-down rate and reduce the cooling time, the additional cooling benefit becomes smaller at higher operating speeds while the energy demand continues to increase noticeably. This behavior indicates diminishing returns in thermal performance at maximum pump operation. Therefore, operating both the cold and battery pumps at balanced moderate-to-high speeds can provide efficient battery cooling performance while limiting excessive energy consumption in the battery cooling mode layout.

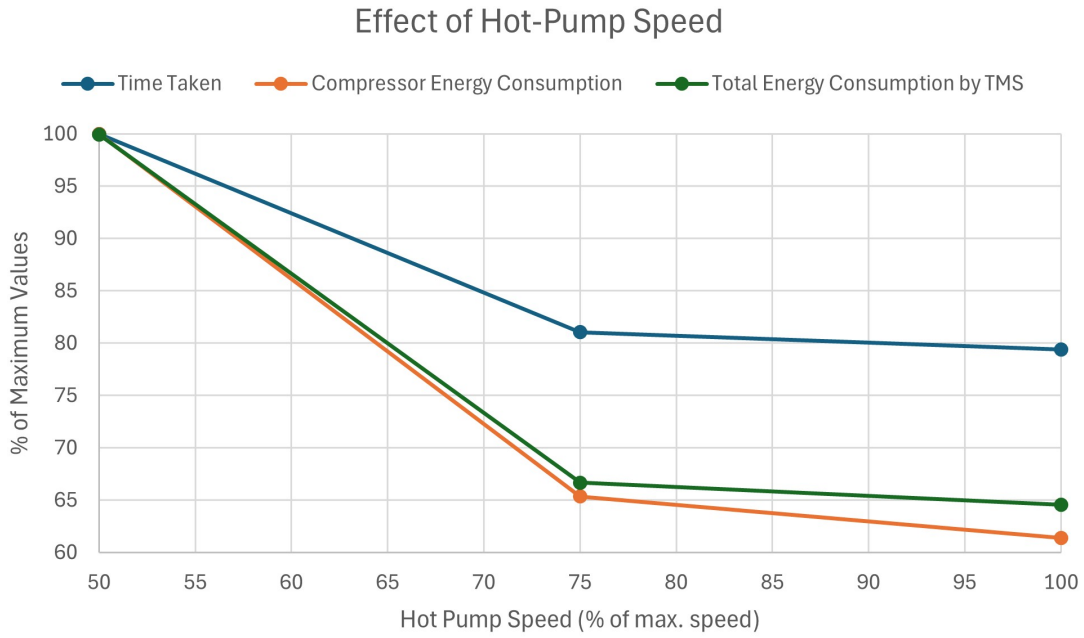

Figure 4.13: Effect of hot-pump speed for battery cooling mode.

Figure 4.13 shows that increasing the hot pump speed improves battery cooling performance by enhancing heat rejection through the WCond and radiator loop. As the hot pump speed increases from 50% to 75%, the time required for battery cooling, compressor energy consumption, and total TMS energy consumption all decrease significantly. Further increasing the hot pump speed to 100% continues to reduce compressor energy and total system energy consumption, although the reduction in cooling time is comparatively smaller.
This indicates that, for battery cooling, stronger hot-side coolant circulation helps the refrigerant loop reject heat more effectively. As a result, the compressor requires less work, and the overall energy consumption of the TMS decreases. Therefore, 100% hot pump speed is preferred for battery cooling when the objective is to minimize

total energy consumption and improve system efficiency.

4.2.2 Battery Cooling Strategy Results for High COP and Low Energy Consumption

Table 4.4: Pump speed settings for different energy efficient battery cooling cases

Case	Battery Pump (%)	ED Pump (%)	Cold Pump (%)	Hot-side Pump (%)	Description
Case 1	50	75	50	100	Best energy-saving case
Case 2	50	75	75	100	Selected energy-efficient case
Case 3	50	100	50	100	Selected energy-efficient case
Case 4	75	75	50	100	Selected energy-efficient case
Case 5	75	75	75	100	Selected energy-efficient case
Case 6	100	100	100	100	Reference: all pumps at maximum speed

The table 4.4 shows the selected battery cooling pump speed combinations used for the WLTC simulation at 40 °C ambient temperature. Compared with the reference case, where all pumps operate at 100% speed, the selected cases use reduced pump speeds to lower auxiliary power consumption.

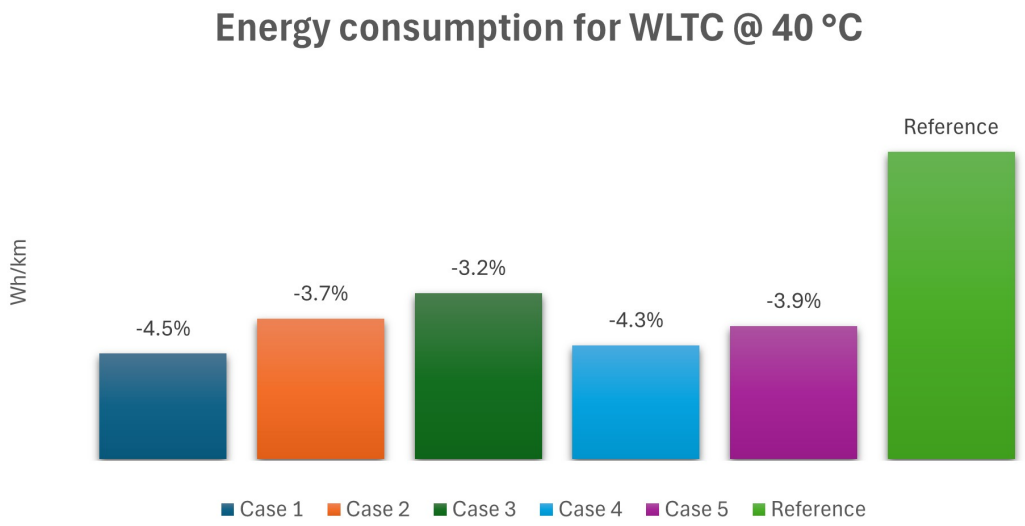

Figure 4.14: Comparison of WLTC energy consumption for different cases during battery cooling mode at 40 °C ambient temperature.

Figure 4.14 shows that all selected cases reduce energy consumption compared with the reference. Case 1 gives the best result, with about 4.5% energy saving, making it the most efficient battery cooling case. This indicates that effective cooling can be achieved without operating all pumps at maximum speed, improving overall vehicle efficiency.

Table 4.5: Proposed pump speed control strategy for battery cooling mode

Battery Temperature	Battery Pump (%)	Cold Pump (%)	ED pump (%)	Hot-side Pump (%)	Description
Fast Charging	75	75	75	100	Fast battery temperature pulldown
$T_{bat} > 35°C$	75	75	75	100	Fast battery temperature pulldown
$T_{bat} \leq 35°C$	50	50	75	100	Efficient battery temperature pulldown

The proposed battery cooling strategy controls the pump speeds based on the battery temperature. When the battery temperature is above 35 °C, the battery pump and cold pump operate at 75% speed to provide fast battery temperature pulldown. This mode is also used during fast charging, where higher heat generation requires quicker cooling.

When the battery temperature is 35 °C or below, the battery pump and cold pump operate at 50% speed to reduce auxiliary power consumption while still maintaining effective battery cooling. The ED pump remains at 75% speed, and the hot-side pump remains at 100% speed in both conditions.

Once the battery temperature reaches 25 °C, the battery cooling mode is switched off to avoid unnecessary cooling energy consumption. Cooling remains off until the battery temperature rises to 35 °C again, after which the cooling mode is reactivated.

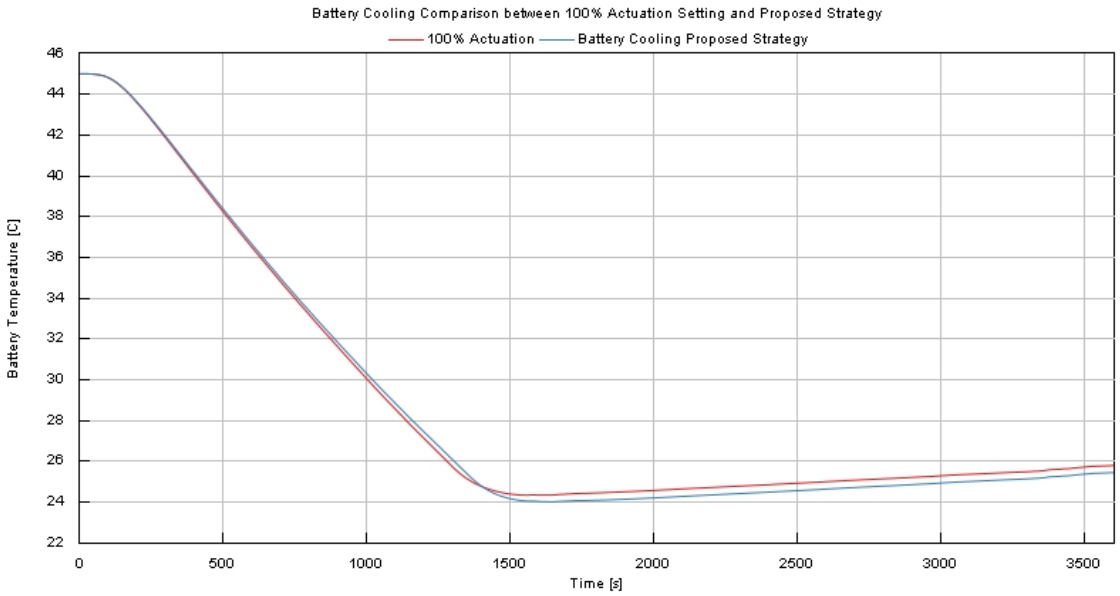

Figure 4.15: Comparison of proposed strategy with 100% actuation strategy for battery cooling test carried under 2XWLTC cycle

Figure 4.15 illustrates that when the proposed strategy is tested under 2 X WLTC cycle the cabin cooling performance of the proposed strategy is almost similar to that if all the pumps are run at maximum speed. But with the proposed strategy we can save the energy consumed by auxiliary components if TMS system by 4.15%.

4.3 Combined Cooling Results

A separate flow survey was performed for the combined cabin–battery cooling mode because coolant distribution changes when both cooling demands are active at the same time (as illustrated in Section 3.3.3). In this mode, sufficient flow must be maintained in both the cabin cooling loop and the battery cooling loop. Therefore,

only cases satisfying the minimum flow requirement in the cabin cooler, battery, hot pump and ED pump were selected for transient thermal analysis. The detailed combined cooling flow survey results are presented in A.3. Out of total 256 cases, 63 cases were selected for the thermal simulation.

4.3.1 Combined Cooling Strategy Results for Efficient Cooling Performance.

Table 4.6 summarizes the actuator speed selection strategy used for combined cabin–battery cooling mode. Since both cabin and battery cooling loads are active simultaneously, the cold-side pump is operated at a minimum of 75% to ensure sufficient chilled coolant supply to both loops. The hot-side pump is fixed at 100% to support maximum heat rejection through the WCond and radiator loop. The ED pump is maintained at 75% or 100% based on the flow survey to avoid hydraulic dominance and ensure stable radiator-side coolant circulation. The battery pump speed is varied depending on whether the control priority is faster battery cooling, balanced cooling, or cabin-prioritized cooling operation.

Table 4.6: Actuator speed selection strategy for combined cabin–battery cooling mode

Actuator	**Selected Speed**	**Reason for Selection**	**Control Purpose**
Cold-pump	Minimum 75%	Combined cooling requires chilled coolant for both the cabin cooler and battery loop. Based on cabin cooling results, higher cold-side flow improves heat removal from the cabin.	Ensure sufficient chilled coolant supply to cabin and battery circuits
Hot-pump	100%	Both cabin and battery loads reject heat through the WCond and radiator loop. Higher hot-side pump speed improves heat rejection and reduces compressor workload.	Maximize heat rejection during combined cooling
ED pump	75% or 100%	Flow survey showed that higher ED pump speed helps maintain stable radiator-side flow and avoids hydraulic dominance between ED and hot-side circuits.	Maintain adequate coolant flow through radiator-side circuit
Battery pump	Varied based on priority	Battery pump speed depends on whether the priority is faster battery cooling, balanced cooling, or cabin-prioritized cooling operation.	Control battery cooling rate and energy consumption

Table 4.7 presents the selected operating case for energy-efficient combined cooling. The thermal simulation confirmed that this actuator combination achieved the highest COP while managing simultaneous heat rejection from both the cabin and battery circuits.

Table 4.7: Maximum-COP actuator setting for combined cooling

Actuator	Speed
Battery pump	50%
Cold pump	75%
ED pump	75%
Hot pump	100%

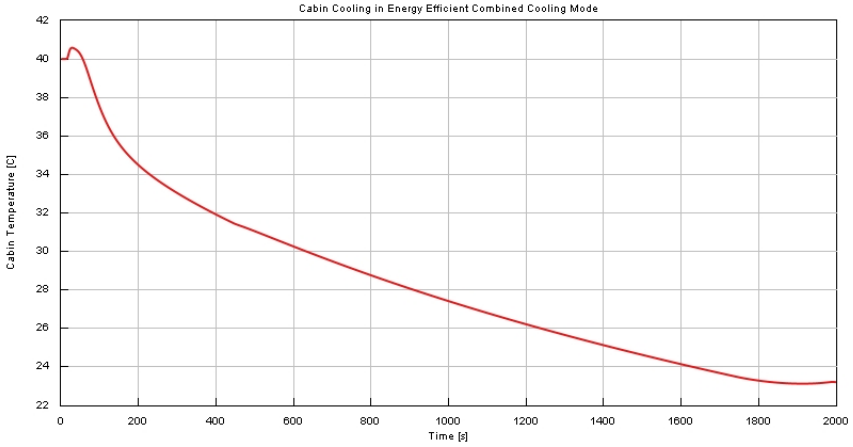

(a) Cabin temperature response

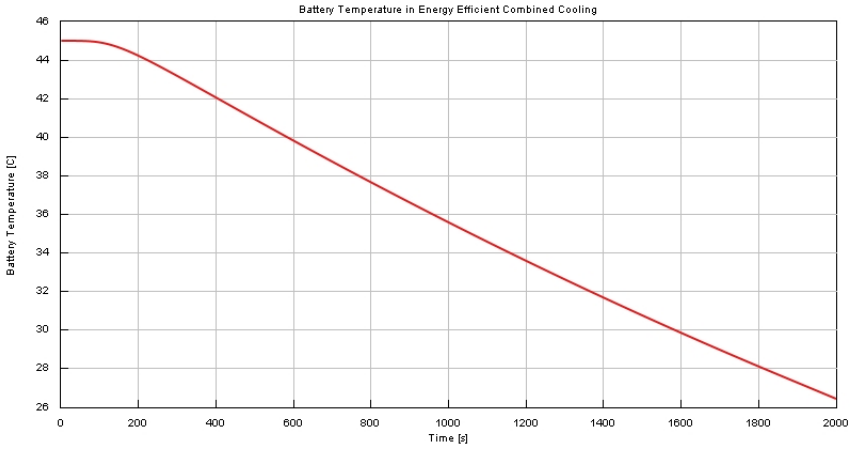

(b) Battery temperature response

Figure 4.16: Cabin and battery temperature response during energy-efficient combined cooling mode

Figure 4.16 shows the cabin and battery temperature responses for the selected energy-efficient combined cooling case. The cabin temperature decreases gradually and requires more time to reach the target temperature because the cooling capacity is shared between the cabin and battery loops. At the same time, the battery temperature decreases continuously, showing that sufficient cooling is maintained for the battery circuit. This confirms that the selected case prioritizes high COP and lower energy consumption rather than rapid cabin pull-down. Therefore, this operating mode is suitable for steady or normal combined cooling opera-

tion, while a cabin-prioritized strategy is required when faster cabin cooling is needed.

4.3.2 Combined Cooling Strategy 2: Faster Cabin Cooling with Slow Battery Cooling

In this strategy, the pump-speed combination from the efficient combined cooling case is retained, but the valve proportionality is adjusted to direct a larger portion of chilled coolant toward the cabin cooler core. The valve opening toward the battery loop is reduced in VMA 1 (Figure 3.5), which limits the coolant flow to the battery circuit and allows more cooling capacity to be supplied to the cabin. Since the battery receives lower coolant flow in this mode, the battery temperature reduction becomes slower. However, this is acceptable when rapid passenger comfort is the main priority and the battery temperature remains within a manageable range.

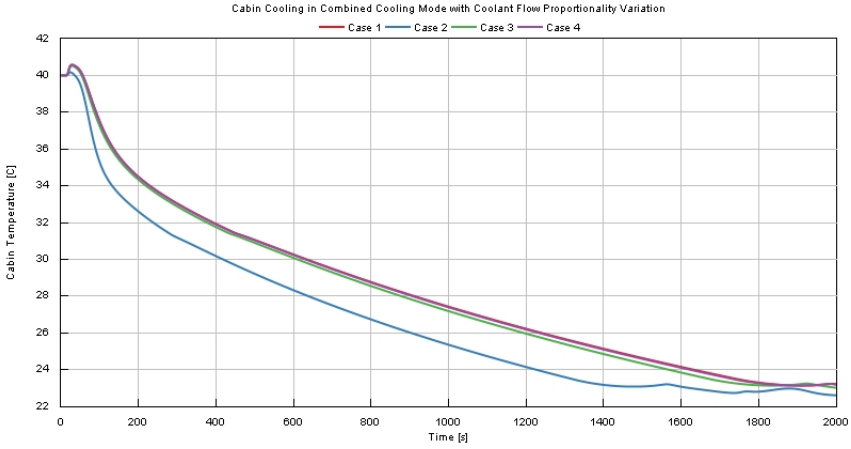

(a) Cabin temperature response

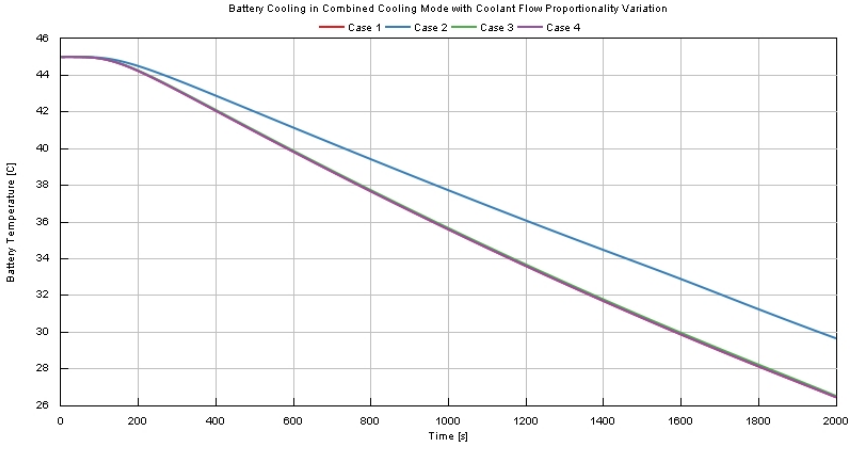

(b) Battery temperature response

Figure 4.17: Effect of battery-side valve proportionality on cabin and battery temperature during cabin-prioritized combined cooling

Figure 4.17 compares the cabin and battery temperature responses for different battery-side valve proportionality settings during combined cooling operation. Case

1 represents the baseline condition (same as efficient combined cooling pump speeds), where no proportionality change is applied and all valve ports remain open. In Cases 2, 3, and 4, the battery-side valve proportionality is set to 25%, 50%, and 75%, respectively, to evaluate how coolant distribution affects cabin and battery cooling performance.

The cabin temperature response shows that Case 2 provides the fastest cabin pull-down. This is because 25% battery-side valve proportionality restricts the coolant flow toward the battery loop, allowing a larger portion of chilled coolant to be directed toward the cabin cooler. However, keeping the battery-side proportionality to 50% and 75% does not improve cabin cooling. Instead, the response becomes closer to the baseline case because more coolant is distributed toward the battery loop.

Since the battery-side valve proportionality is reduced to 25%, only a limited amount of chilled coolant from the chiller is directed toward the battery loop. Under this condition, operating the battery pump at high speed may not provide a significant improvement in battery cooling, because the available coolant flow to the battery circuit is already restricted by the valve proportionality. Instead, higher battery pump speed would mainly increase auxiliary energy consumption. Therefore, the required battery pump speed is analyzed separately for this cabin-prioritized combined cooling condition to identify the minimum pump operation that can maintain acceptable battery cooling while improving overall energy efficiency.

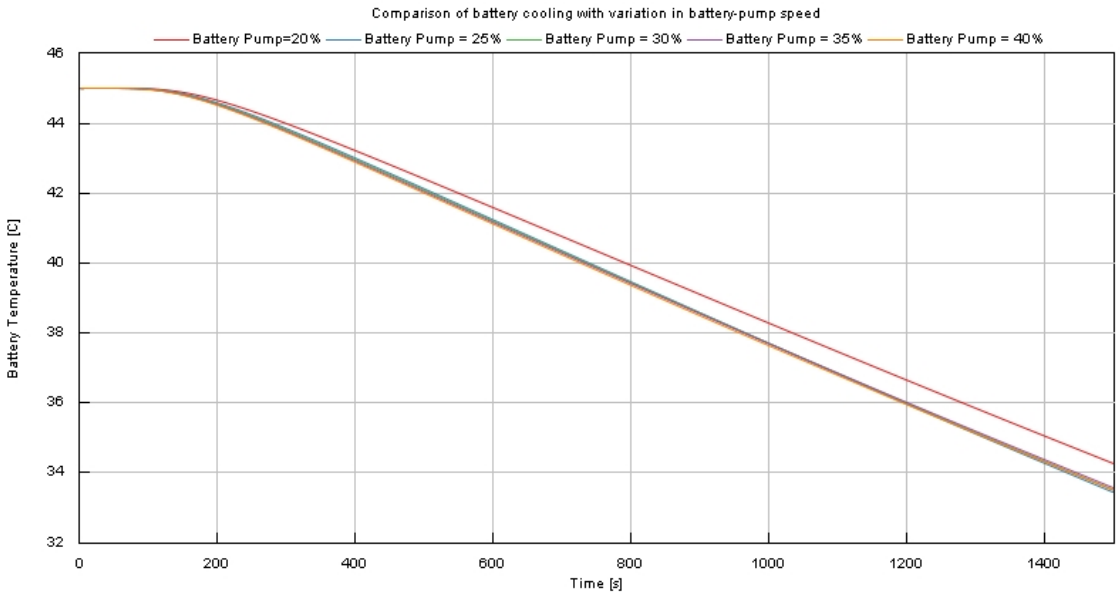

Figure 4.18: Comparison of battery pump speeds for combined cooling prioritizing cabin cooling

The results in Figure 4.18 show that the battery temperature reduction is very similar for pump speeds above 25%. The curves for 25%, 30%, 35%, and 40% are close to each other, indicating that higher battery pump speeds provide only marginal

additional cooling. Since the valve proportionality is fixed for cabin-prioritized operation, the coolant flow directed toward the cabin cooler remains unchanged. Therefore, the cabin cooling response is expected to remain nearly the same for all battery pump speed conditions. Hence, 25% battery pump speed is sufficient for this operating condition, as it maintains gradual battery cooling without affecting cabin cooling performance and avoids unnecessary pump energy consumption.

4.3.3 Combined Cooling Strategy 3: Prioritized Battery Cooling With Cabin Cooling

Based on the thermal simulation results, the best operating condition for the battery-prioritized combined cooling mode was obtained with 75% cold pump speed, 75% battery pump speed, 100% hot pump speed, and 75% ED pump speed. In this case, the fully opened battery-side flow path and higher battery pump operation increase coolant circulation through the battery loop, improving battery heat removal. At the same time, the cold pump operates at 100% to provide sufficient chilled coolant to support both battery and cabin cooling. The hot pump is maintained at 100% to ensure strong heat rejection through the WCond and radiator loop, while the ED pump operates at 75% to maintain stable radiator-side flow. This actuator combination provides stronger battery cooling while still allowing cabin cooling to continue during combined operation.

Table 4.8: Temperature-based selection of combined cabin–battery cooling strategies

Combined Cooling Mode	**Temperature Condition**	**When to Use**	**Main Setting**
Energy-efficient combined cooling	Cabin near target: 23–25°C; Battery < 40°C	Normal combined cooling or steady operation	Battery pump: 50%; Cold pump: 75%; ED pump: 75%; Hot pump: 100%
Cabin-prioritized combined cooling	Cabin > 25°C; Battery < 40°C	Faster cabin pull-down while battery cooling continues slowly	Battery-side valve proportionality: 25%; Battery pump: 25%; Cold pump: 75%; ED pump: 75%; Hot pump: 100%
Battery-prioritized combined cooling	Battery ≥ 40°C; Cabin cooling still required	Fast charging or high battery thermal load with cabin cooling demand	Battery-side flow path: 100% open; Battery pump: 75%; Cold pump: 75%; ED pump: 75%; Hot pump: 100%

Table 4.8 presents the temperature-based selection logic for the combined cabin–battery cooling strategies.This strategy is used to prevent the thermal management system from operating with a single fixed actuator setting under all combined cooling conditions. Since cabin comfort and battery protection have different thermal requirements, the cooling priority must change depending on the operating condition. Cabin-prioritized cooling improves passenger comfort during high cabin temperature conditions, while battery-prioritized cooling protects the battery when it approaches the critical temperature limit. Once both requirements are satisfied, the system can shift to energy-efficient operation to reduce auxiliary power consumption and improve COP. This priority-based strategy therefore allows the system to balance comfort, safety, and energy efficiency during combined cooling operation.

5

Conclusion

5.1 Summary

This thesis investigated the cooling performance and actuator operating strategy of a full-secondary-loop thermal management system for a battery electric vehicle. The study focused on cabin cooling, battery cooling, and combined cabin–battery cooling modes, with particular attention to the operation of coolant pumps, radiator fan, and heat rejection through the WCond–radiator loop. The aim was to identify operating strategies that can provide effective thermal control while reducing unnecessary auxiliary energy consumption and improving system COP.

The results show that actuator settings strongly influence system performance. Higher pump and fan speeds generally improve coolant circulation and heat rejection, but they also increase auxiliary energy demand. Therefore, the most effective strategy is not continuous maximum-speed operation, but mode-dependent actuator control based on thermal load, ambient condition, and vehicle speed.

For cabin cooling, 75% cold-side pump speed provided the best balance between faster pull-down and energy use. A lower cold pump speed reduced energy consumption but slowed cabin cooling, while 100% pump speed gave only limited additional cooling benefit with higher energy demand. The WCond pump improved heat rejection and reduced compressor work, especially at higher ambient temperature. Based on this, a two-stage cabin cooling strategy is recommended: fast pull-down during initial cooling, followed by energy-efficient operation near the target temperature.

For battery cooling, 75% battery pump and 75% cold-side pump operation improved battery temperature reduction. Since the battery has high thermal mass, cooling response is slower and sustained heat removal is required. The hot-side pump played a major role by improving heat rejection through the WCond and radiator loop. Higher hot-side pump speed reduced compressor effort and improved overall cooling efficiency.

For combined cabin–battery cooling, the thermal load increased because both cooling demands were active at the same time. The flow survey showed that the cold-side pump should operate at a minimum of 75%, the hot-side pump at 100%, and the ED pump at 75% or 100% to maintain stable flow distribution. The thermal simulation confirmed that the highest COP was achieved with 50% battery pump, 75% cold pump, 75% ED pump, and 100% hot pump. This pump-speed combination was then

used as the base operating condition for further valve proportionality analysis.
The valve proportionality was varied based on the cooling priority between the cabin and battery loops, while keeping the main pump speeds unchanged. During cabin-prioritized cooling, only 25% valve opening toward the battery was used so that a larger portion of chilled coolant could be directed to the cabin cooler core, improving cabin pull-down performance. Since the battery receives reduced coolant flow in this condition, the battery pump speed can be decreased to avoid unnecessary auxiliary energy consumption while maintaining the same overall cooling strategy. On the other hand, during battery-prioritized combined cooling the valve opening towards the battery is opened 100% to allow maximum flow towards the battery and the battery-pump speed was kept at 75%.

For WLTC operation, selected energy-efficient cases were compared against the reference case where all pumps operated at full speed. The results showed that reduced pump-speed combinations lowered energy consumption while maintaining acceptable cooling performance. Fan optimization also showed that high fan speed is needed at low vehicle speed, while fan operation can be reduced at higher speeds due to ram-air cooling.

The results support the Chapter 2 discussion on integrated secondary-loop thermal management systems. Literature shows that secondary-loop architectures improve system flexibility and are suitable for refrigerant isolation, especially when low-GWP refrigerants such as R290 are considered. The present study adds to this by showing how actuator operation influences COP and energy consumption in such an architecture. For Volvo and other OEMs, the results suggest that full-secondary-loop systems should use adaptive actuator strategies instead of fixed maximum-speed operation. Pump and fan commands can be calibrated according to cooling mode, ambient temperature, vehicle speed, and component demand. This can improve energy efficiency while maintaining cabin comfort and battery thermal control.

5.2 Future Scope

1. Develop thermal control strategies for a wider range of realistic operating scenarios.
2. Extend the present cooling-mode analysis to heating mode, especially cabin heating, battery warm-up, and heat pump operation under low ambient temperature conditions.
3. Design a dynamic mode selection framework to identify the appropriate modes based on real-time thermal demands.
4. Implement an automatic controller for intelligent switching and prioritization between operating modes.
5. Optimize control operation to achieve maximum energy efficiency while maintaining cabin comfort and battery thermal limits.

6

References

1. IEA (2025), Global EV Outlook 2025, IEA, Paris
   https://www.iea.org/reports/global-ev-outlook-2025, Licence: CC BY 4.0.

2. Chowdhury S., Leitzel L., Zima M., Santacesaria M. et al., “Total Thermal Management of Battery Electric Vehicles (BEVs)", SAE Technical Paper 2018-37-0026, 2018, doi:10.4271/2018-37-0026

3. Mengchen Bai, Naijiang Liu, Jiaxin Liu, Li Li, Weijin Zhang, Martin Kreschel, "A review of thermal management technologies for electric vehicles", Journal of Energy Storage,Volume 143, 2026, 119658, ISSN 2352-152X,
   https://doi.org/10.1016/j.est.2025.119658.

4. Dan, Dan & Zhao, Yihang & Wei, Mingshan & Wang, Xuehui. "Review of Thermal Management Technology for Electric Vehicles.(2023)"
   Energies.16.4693.10.3390/en16124693.

5. Möser, C., and Flack, M., Schaeffler Kolloquium, 2022

6. Muthukrishnan, K., Saikrishna, S., Mahobia, T., and Vijayaraj, J.M., “Design and Analysis on Integrated Thermal Management Solution for Electric Vehicles,” SAE Technical Paper 2025-28-0418, 2025, doi:10.4271/2025-28-0418.

7. Qian Wang, Bin Jiang, Bo Li, Yuying Yan, "A critical review of thermal management models and solutions of lithium-ion batteries for the development of pure electric vehicles", Renewable and Sustainable Energy Reviews, Volume 64, 2016, Pages 106-128, ISSN 1364-0321,
   https://doi.org/10.1016/j.rser.2016.05.033

8. Angelo Maiorino, Claudio Cilenti, Fabio Petruzziello, Ciro Aprea,"A review on thermal management of battery packs for electric vehicles", Applied Thermal Engineering, Volume 238,2024, 122035, ISSN 1359-4311,
   https://doi.org/10.1016/j.applthermaleng.2023.122035

9. Kim, ChaeSil, and NeungGyo Ha. 2025. "A Study on the Vibration and Noise Reduction of Scrolling-Type Electric Compressor for Electric Vehicles" World Electric Vehicle Journal 16, no. 3: 126.
   https://doi.org/10.3390/wevj16030126

10. X. Wang, B. Li, D. Gerada, K. Huang, I. Stone, S. Worrall, Y. Yan, "A critical review on thermal management technologies for motors in electric cars", Applied Thermal Engineering, Volume 201, Part A, 2022, 117758, ISSN 1359-4311, https://doi.org/10.1016/j.applthermaleng.2021.117758

11. James M. Calm, "The next generation of refrigerants – Historical review, considerations, and outlook", International Journal of Refrigeration, 2008, https://doi.org/10.1016/j.ijrefrig.2008.01.013.

12. Panday, A. (2026). "The future of automotive refrigerants: Navigating the regulatory transition." S&P Global Mobility – AutoTechInsight, https://www.spglobal.com/automotive-insights/en/blogs/2026/04/the-future-of-automotive-refrigerants

13. Liange He, Haodong Jing, Yan Zhang, Pengpai Li, Zihan Gu, "Review of thermal management system for battery electric vehicle", Journal of Energy Storage, Volume 59, 2023, 106443, ISSN 2352-152X, https://doi.org/10.1016/j.est.2022.106443

14. Chinnaraj, C. and Govindarajan, P., 2010. "Performance analysis of electronic expansion valve in 1 TR window air conditioner using various refrigerants". International Journal of Engineering Science and Technology, 2

15. J. Bae, J. Yun, and J. Han, "Performance and efficiency evaluation of a secondary loop integrated thermal management system with a multi-port valve for electric vehicles," Energies 2024, 17(22), 5729 https://doi.org/10.3390/en17225729

16. "Thermal Expansion Valve," ForeForums Wiki. [Online]. Available: `https://wiki.foreforums.com/technical:air_conditioning_system:dash:expansion`.

A
Appendix

A.1 Cabin Cooling Case Matrix

Table A.1: Complete actuator case matrix for cabin cooling flow survey

Case	ED Pump (%)	Cold Pump (%)	Hot Pump (%)
1	25	25	25
2	25	25	50
3	25	25	75
4	25	25	100
5	25	50	25
6	25	50	50
7	25	50	75
8	25	50	100
9	25	75	25
10	25	75	50
11	25	75	75
12	25	75	100
13	25	100	25
14	25	100	50
15	25	100	75
16	25	100	100
17	50	25	25
18	50	25	50
19	50	25	75
20	50	25	100
21	50	50	25
22	50	50	50
23	50	50	75
24	50	50	100
25	50	75	25
26	50	75	50
27	50	75	75
28	50	75	100
29	50	100	25
30	50	100	50
31	50	100	75

Case	Cold Pump (%)	ED Pump (%)	Hot Pump (%)
32	50	100	100
33	75	25	25
34	75	25	50
35	75	25	75
36	75	25	100
37	75	50	25
38	75	50	50
39	75	50	75
40	75	50	100
41	75	75	25
42	75	75	50
43	75	75	75
44	75	75	100
45	75	100	25
46	75	100	50
47	75	100	75
48	75	100	100
49	100	25	25
50	100	25	50
51	100	25	75
52	100	25	100
53	100	50	25
54	100	50	50
55	100	50	75
56	100	50	100
57	100	75	25
58	100	75	50
59	100	75	75
60	100	75	100
61	100	100	25
62	100	100	50
63	100	100	75
64	100	100	100

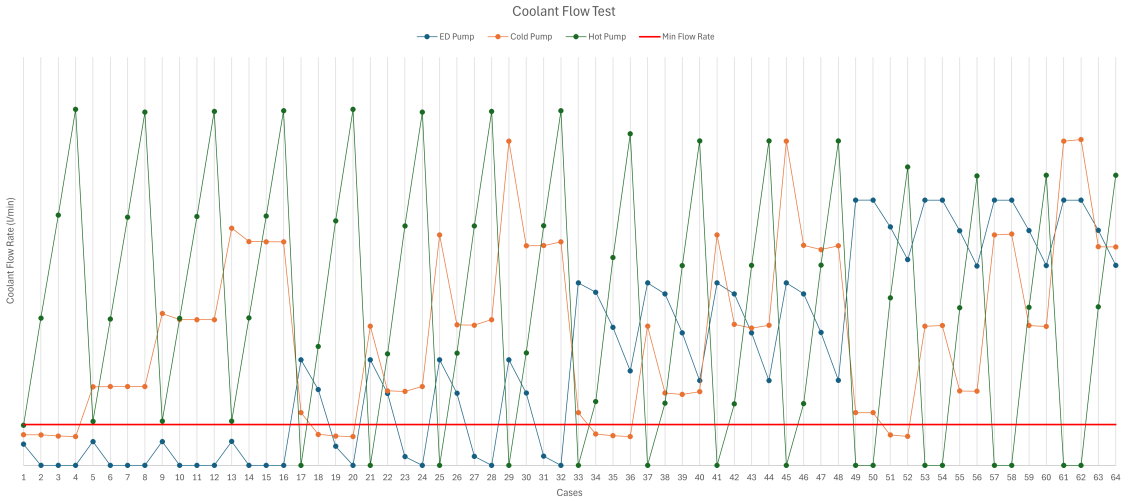

Figure A.1: Flow analysis through various pumps in cabin cooling mode for different cases

A.2 Battery cooling flow test result

In battery-cooling flow simulation, battery pump speed is also varied. The 64 cases are same as cabin-cooling case setup, and this analysis is done by varying the battery pump speed. So total cases for this analysis is 256.

Table A.2: Battery pump speed grouping for the 256 battery cooling flow survey cases

Case Range	Battery Pump Speed (%)
1–64	25
65–128	50
129–192	75
193–256	100

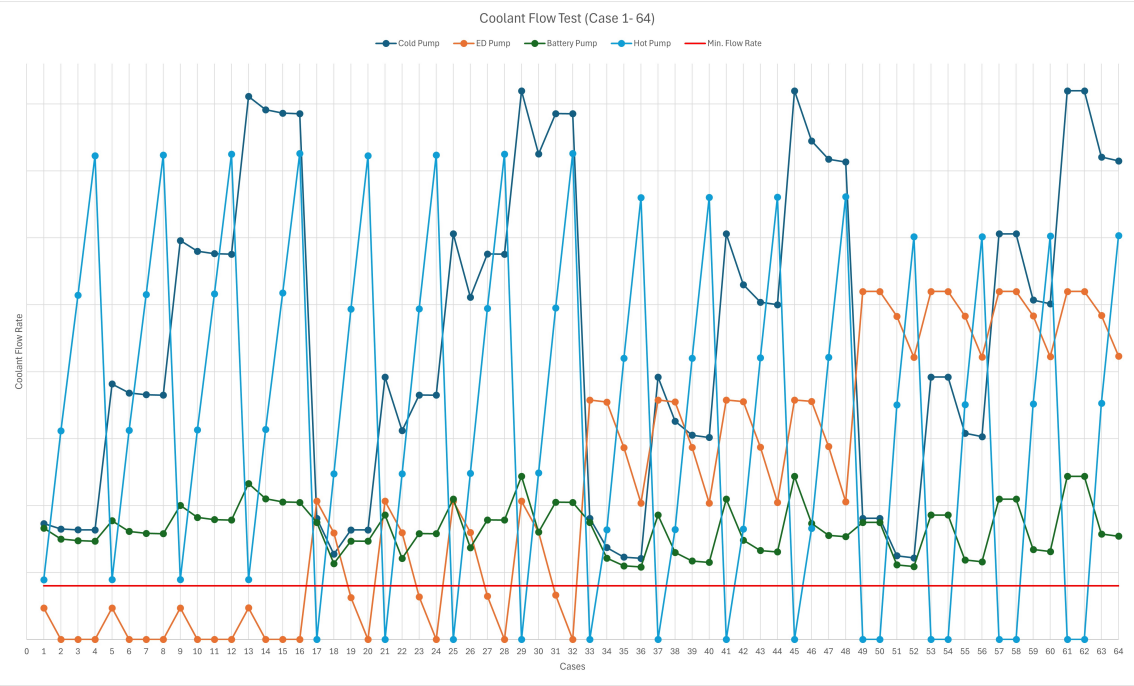

Figure A.2: Flow analysis of coolant in battery cooling mode for cases (1-64)

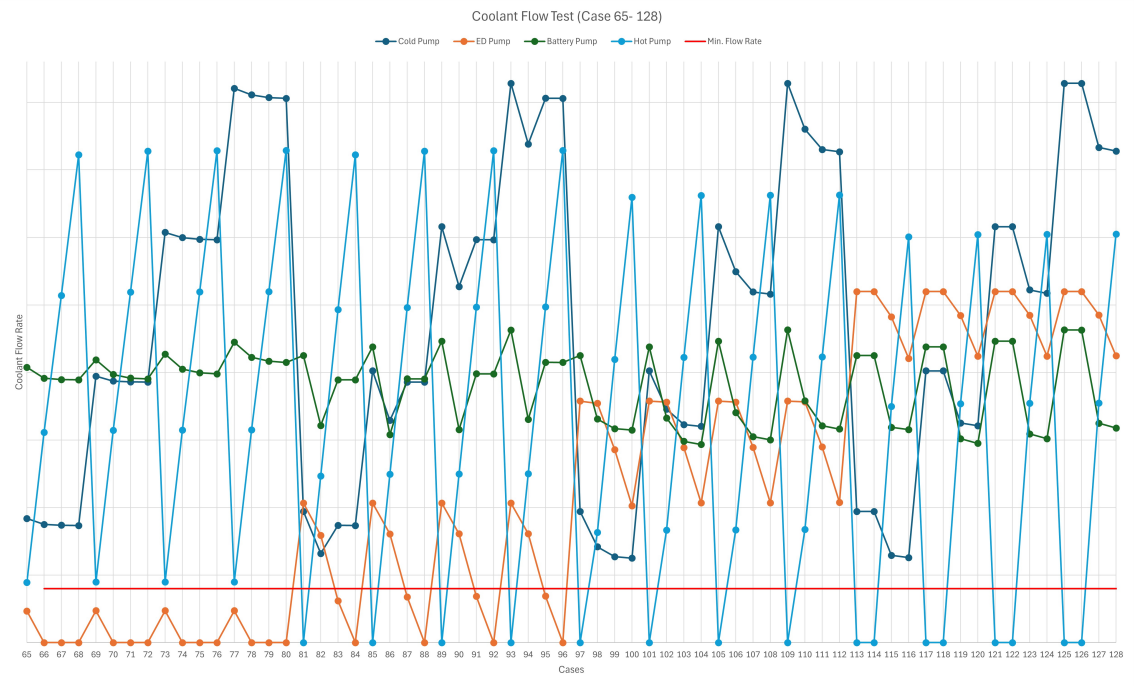

Figure A.3: Flow analysis of coolant in battery cooling mode for cases (65-128)

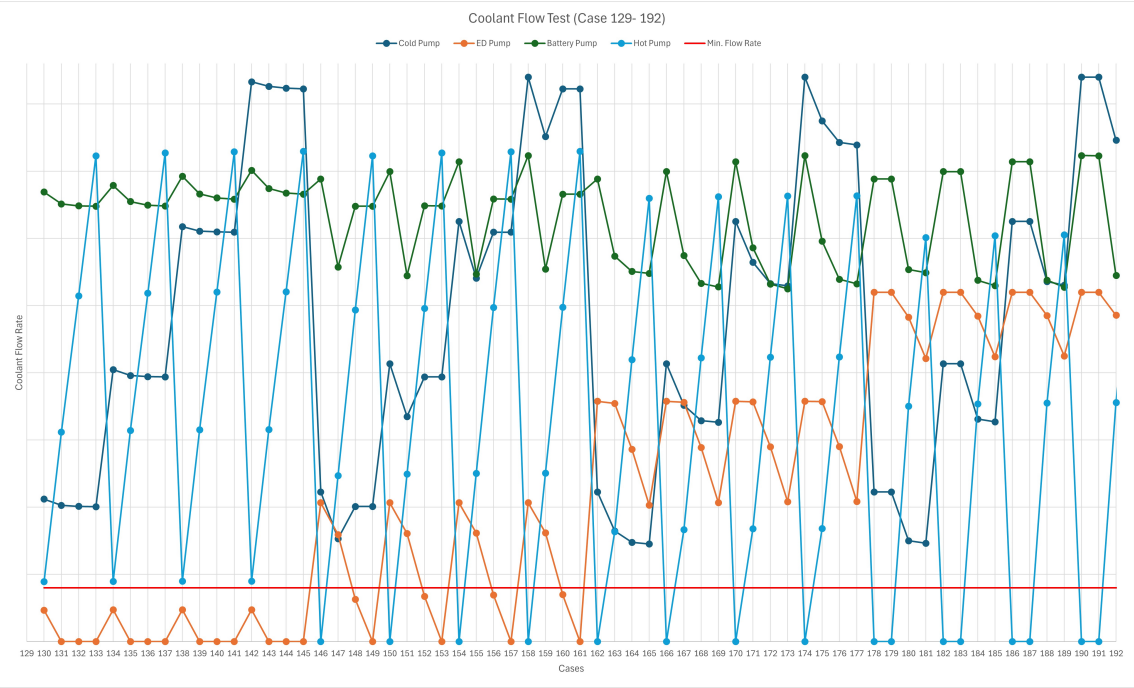

Figure A.4: Flow analysis of coolant in battery cooling mode for cases (129-192)

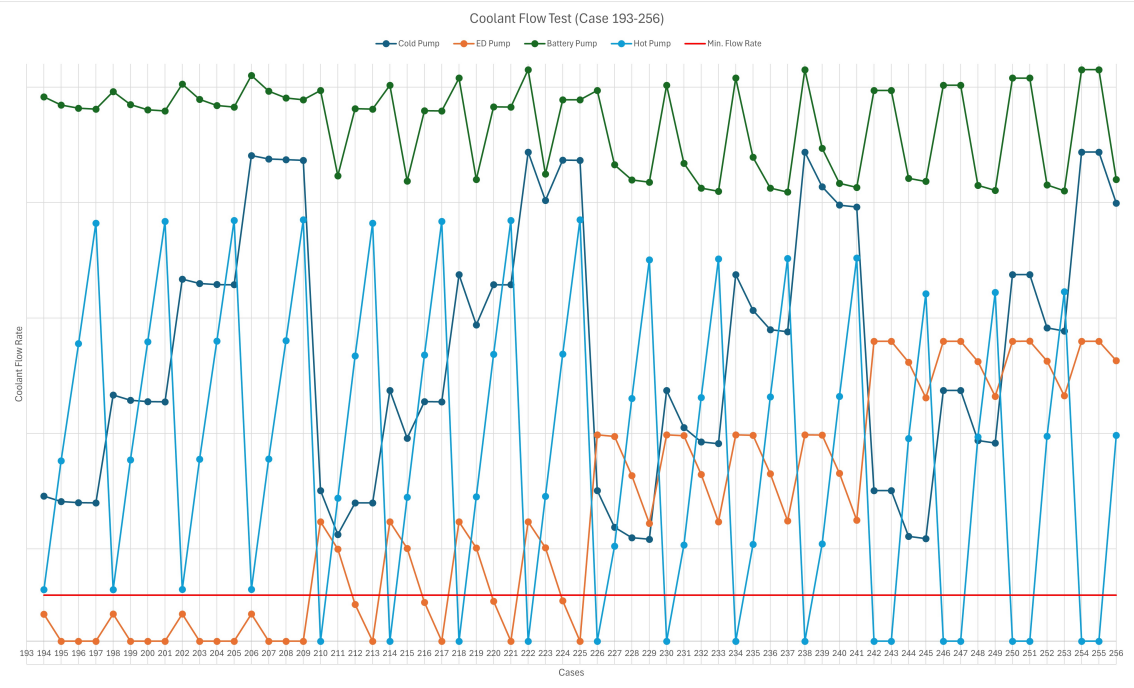

Figure A.5: Flow analysis of coolant in battery cooling mode for cases (193-256)

A.3 Combined cooling flow test result

For combined cooling the cases are same as battery cooling, but we will be analysing the flow in cabin cooler instead of flow in chiller in this mode.

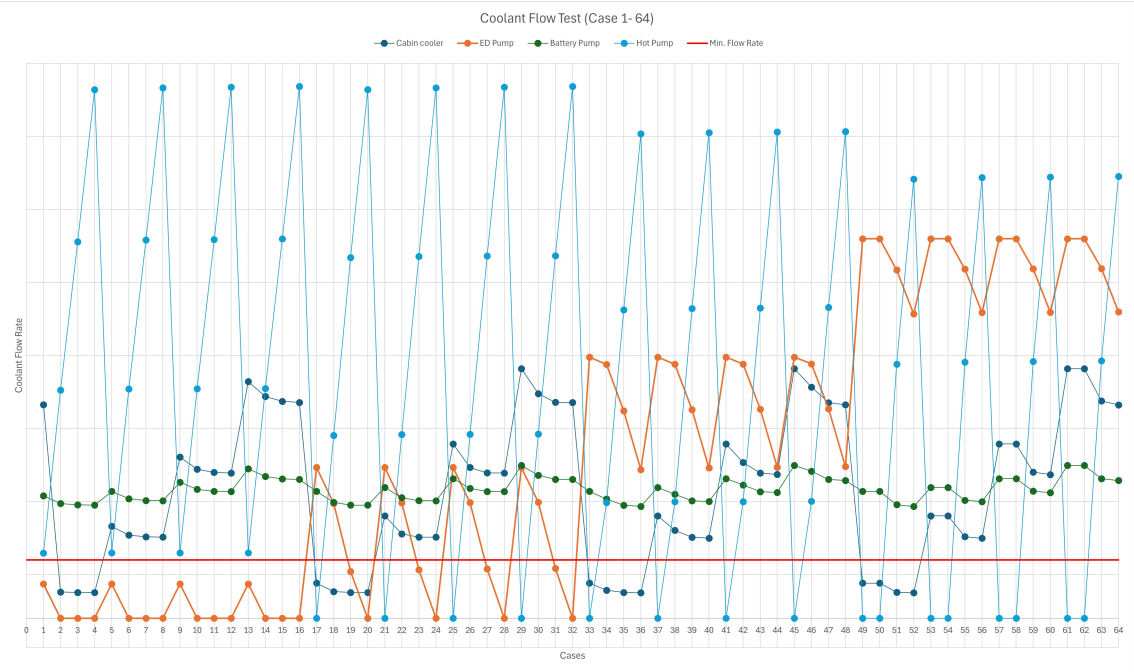

Figure A.6: Flow analysis of coolant in combined cooling mode for cases (1-64)

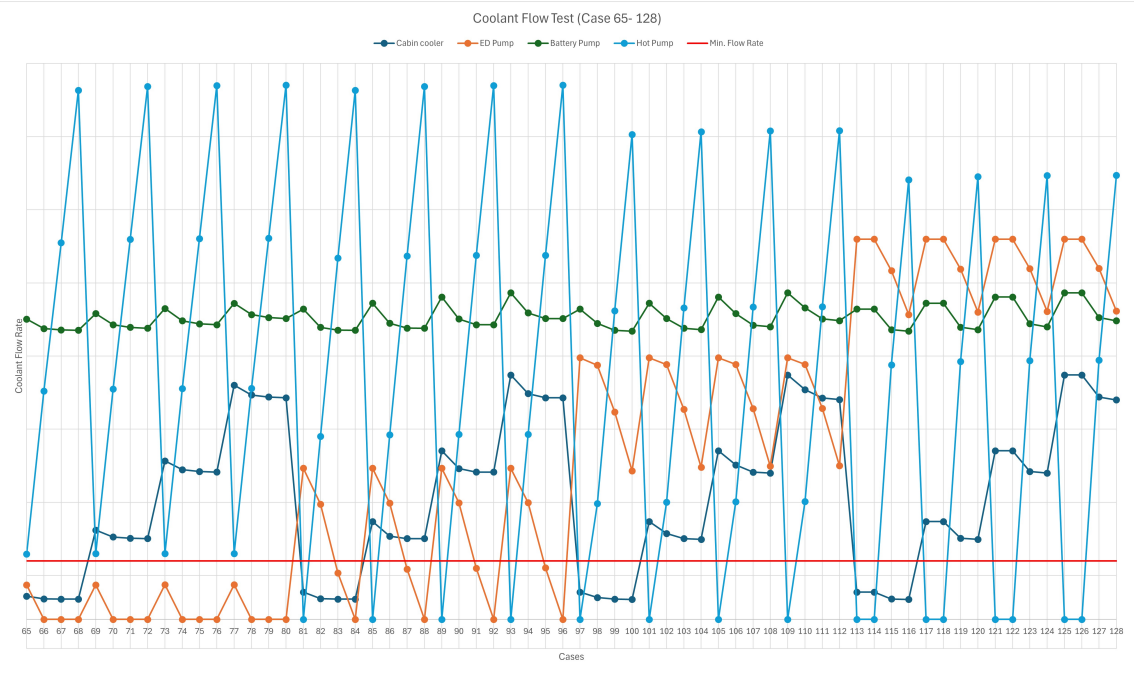

Figure A.7: Flow analysis of coolant in combined cooling mode for cases (65-128)

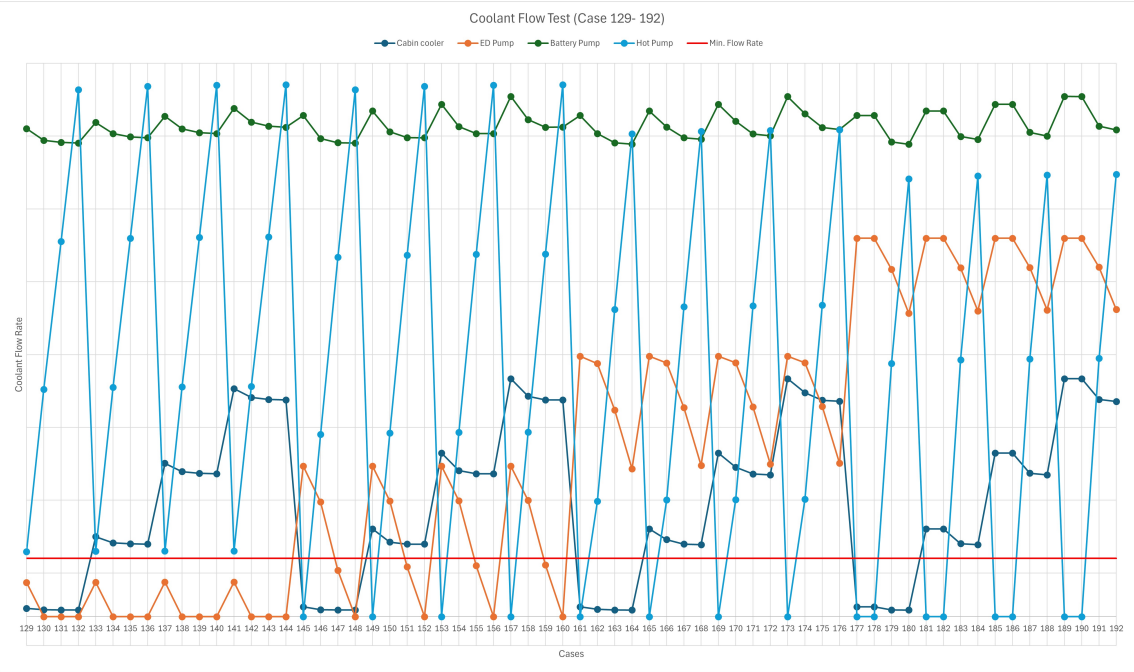

Figure A.8: Flow analysis of coolant in combined cooling mode for cases (129-192)

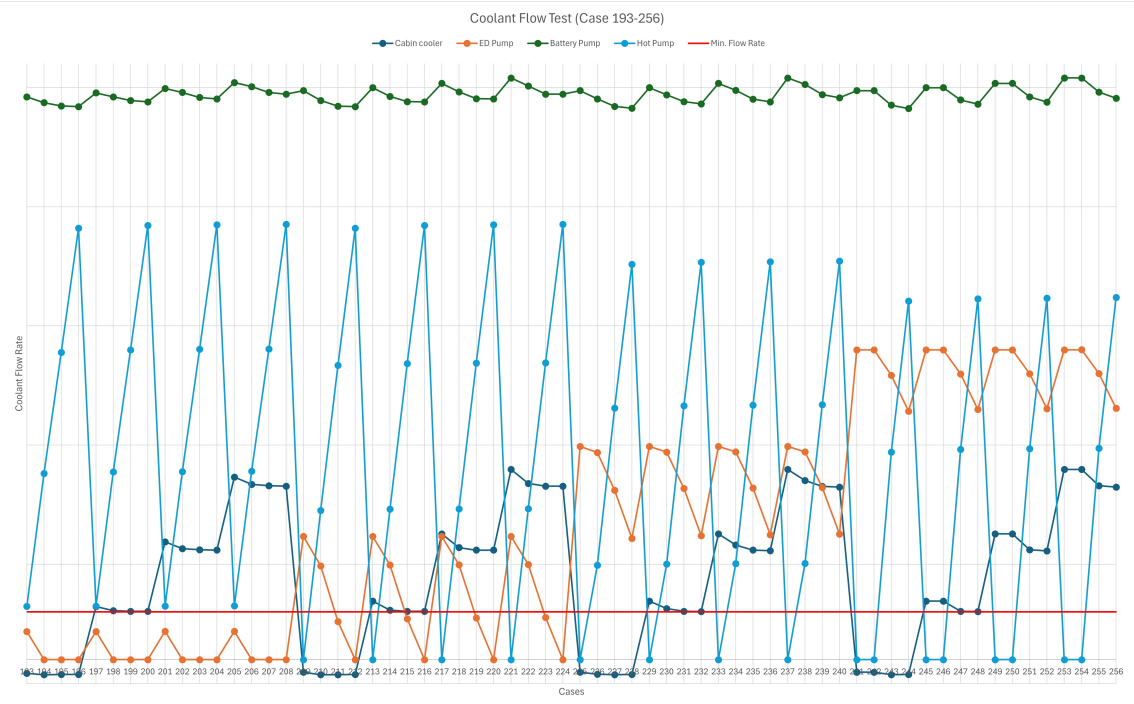

Figure A.9: Flow analysis of coolant in combined cooling mode for cases (193-256)

DEPARTMENT OF SOME SUBJECT OR TECHNOLOGY
CHALMERS UNIVERSITY OF TECHNOLOGY
Gothenburg, Sweden
www.chalmers.se

CHALMERS
UNIVERSITY OF TECHNOLOGY